

Theory of thermophoresis. II. Low-density behavior

Isaac Goldhirsch

Department of Chemistry, Massachusetts Institute of Technology, Cambridge, Massachusetts 02139

David Ronis

Department of Chemistry, Harvard University, Cambridge, Massachusetts 02138

(Received 29 December 1981)

Kinetic theory, in the repeated-ring approximation, is employed to calculate the general expressions for thermophoretic forces and velocities which were obtained in the preceding paper (I). The velocity is not renormalized by the repeated-ring terms, since they all cancel. The thermophoretic force, on the other hand, is strongly renormalized by these terms, since the friction constant is. The latter changes from Boltzmann-type behavior at low densities of the host gas to Stokes-type behavior. In the limit in which the guest particle is represented by a hard-sphere potential we regain known results in the Boltzmann regime. These results are at variance with experiment. A realistic attractive tail, added to the hard-sphere potential yields a vanishingly small correction because of the typical short ranges of such tails. When accommodation processes are included, one obtains excellent agreement with experiment, provided the longitudinal and transverse momentum have different accommodation coefficients.

I. INTRODUCTION

In the preceding paper,¹ denoted by I, we have developed a general formalism for the phenomenon of thermophoresis. We obtained molecular expressions for both the thermophoretic force and velocity. The thermophoretic force coefficient was shown to be related in a simple manner to the Soret coefficient. The mode-coupling renormalization of the Soret coefficient was shown to be negligibly small with respect to its observed values. We concluded that the Soret coefficient was basically given by its "bare" value and therefore one needs a microscopic calculation to obtain this value.

Since the relevant experiments² are mostly performed on aerosols or small particles in host gases, and since the only microscopic approach at hand is provided by kinetic theory,³ we employ this theory for the calculation of the thermophoretic force coefficient. We use the repeated-ring approximation⁴ which is known to yield good results for a large range of gas densities.

It turns out that the thermophoretic velocity is unaffected by the repeated ring terms. They all cancel. On the other hand, the thermophoretic force is strongly renormalized by those terms. They are responsible for the crossover of the friction from its Boltzmann value to the Stokes value. The

fact that our theory compares well with experiment can be taken as support for the repeated ring approximation for the friction coefficient.⁵

An inspection of the type of terms that contribute to thermophoresis shows that they are of a nonhydrodynamic nature, thus confirming the same statement we made in I, based on the mode-coupling analysis. As we shall show, the kinetic theory calculation presented here gives a result for the diffusion constant and thermal-diffusion ratio which has exactly the form obtained in I. The only difference is the fact that the bare quantities are known in kinetic theory and hence numerical values for the thermophoretic force and steady velocity can be computed and compared with experiment.

The meaning of this result is that the main processes that are "responsible" for thermophoresis occur close to the surface of the guest particle (on a length scale which is "invisible" to hydrodynamics). The surface processes are either "reversible" or "irreversible." By the former we mean potential scattering events. The latter are responsible for accommodation processes and reflect the coupling of the host particles to the internal degrees of freedom of the guest particle. A realistic potential between a typical guest particle (of linear size $1 \mu\text{m}$) and a host particle is a hard sphere with a short attractive tail. The range of such a tail is of the order of

angstroms. As a result, we can show that this tail is unimportant for integrated cross sections (which we need for the calculation of thermophoretic coefficients). Thus, as far as the potential is concerned, a hard sphere is sufficient. Such a potential has been used in all previous kinetic calculations. Since the hard-sphere calculations disagree with experimental data, we need to take into account accommodation processes. It turns out that energy accommodation cannot account for the experimental findings⁶; neither can a diffuse scattering term.⁷ We employ a momentum accommodation mechanism, with different accommodation coefficients for transverse and longitudinal components. Such a model has been shown to give good fit to atom-surface scattering data.⁸ It turns out that this model is in quantitative agreement with the available thermophoresis data as well.

This paper is organized as follows. Section II shows how to specialize the results of paper I to the case of a "dilute" host gas. In Sec. III a short introduction to modern kinetic theory is provided and the expressions needed for our purposes, in the repeated ring approximation, are derived. Section IV is devoted to the actual calculation of these terms. Our main approximations are made there. The results of Sec. IV are used in Sec. V to compare to experimental data. Section VI provides a discussion of our results, the approximations involved in obtaining them, as well as necessary future work.

II. SPECIALIZATION OF THE GENERAL THEORY TO LOW DENSITIES

As was shown in Sec. II of paper I, the thermophoretic force constant, through its dependence on the thermal-diffusion ratio, depends on the following quantities:

$$\tilde{V}_T \equiv \int_0^\infty dt \frac{\langle \vec{P}_B(t) \vec{I}_{E,F}(0) \rangle}{M k_B T^2} \quad (2.1)$$

and the friction coefficient ξ ,

$$\xi^{-1} \equiv \int_0^\infty dt \frac{\langle \vec{P}_B(t) \vec{P}_B \rangle}{M^2 k_B T}, \quad (2.2)$$

which gave [cf. Eq. (2.46) of paper I (I2.46)] the thermal-diffusion ratio, and

$$k_T = \xi \tilde{V}_T / k_B \quad (2.3)$$

and [cf. Eq. (I2.30)] gave the thermophoretic force constant:

$$\eta_T = \xi \tilde{V}_T - k_B. \quad (2.4)$$

The significance of \tilde{V}_T is easily seen by solving the equation of motion [Eq. (I2.29)] for the "B" particle's steady-state velocity at constant pressure. We thereby obtain

$$\vec{V}_B = - \left[\tilde{V}_T - \frac{k_B}{\xi} \right] \vec{\nabla} T. \quad (2.5)$$

The term in k_B in Eq. (2.5) is completely negligible, and hence \vec{V}_T is the large-particle velocity per unit $\vec{\nabla} T$.

A final comment: \tilde{V}_T and ξ^{-1} as defined by Eqs. (2.1) and (2.2) are simply the Soret coefficient and diffusion constant (up to trivial factors of $k_B T$) considered in the preceding paper. The reason for the new notation (and that is all that has been introduced) is to facilitate a comparison with experiment. The plan of the calculation is exactly as in the phenomenological mode-coupling approach presented in Sec. III of I. Thus, the transport coefficients are calculated (i.e., \tilde{V}_T or $L_{B,T}$ and ξ^{-1} or D) and from these the thermophoretic force, velocity, etc., are computed.

As was shown in Sec. III of I, the Soret coefficient (and thus \tilde{V}_T) could not be computed via purely macroscopic arguments. In order to understand the phenomena of thermophoresis, we are thus forced to consider some microscopic details.

At present, the only systems for which such details can be included analytically in a semirigorous way are gases (we ignore the molecular dynamics methods). Therefore, we now use kinetic theory to calculate \tilde{V}_T and ξ .

In order to carry out the kinetic calculations, we make some simplifying assumptions: First, the terms in $\vec{I}_{E,F}$ (Ref. 1) explicitly containing the potentials and interparticle forces are dropped. There are two reasons for this. They come in as higher-order density corrections and more importantly, require a pair of particles to be close together, a situation which does not last for very long times. Thus there should be no new singular density dependence associated with these terms. This is in contradistinction to changes in momentum which persist for much longer times. Thus the dissipative heat current is taken to be

$$\vec{I}_{E,F} = \sum_{j \in f} \left[\frac{\vec{p}_j^2}{2m} - \frac{5}{2} k_B T \right] \frac{\vec{p}_j}{m}, \quad (2.6)$$

where we have introduced the low-density form for the enthalpy [cf. (I2.41)]. For the purpose of com-

puting Eq. (2.1), the identity of the fluid particles can be used to rewrite \tilde{V}_T as

$$\tilde{V}_T = \frac{\rho_f \mathcal{V}}{m M k_B T^2} \int_0^\infty dt \left\langle \tilde{\mathbf{P}}_B(t) \left[\frac{p_2^2}{2m} - \frac{5}{2} k_B T \right] \frac{\tilde{\mathbf{p}}_2}{m} \right\rangle, \quad (2.7)$$

where "2" is a typical gas particle and \mathcal{V} is the system volume. The second assumption is the use of an ideal gas distribution function in evaluating the averages. That is,

$$f(X^{\mathcal{N}})_{\text{eq}} \approx \frac{1}{\mathcal{V}^{\mathcal{N}}} \prod_j \phi_j(p_j), \quad (2.8)$$

where ϕ_j is a Boltzmann momentum distribution for the j th particle and $\mathcal{N}-1$ is the number of gas particles. Both of these approximations are not essential and can be corrected using standard techniques. The consequences of Eqs. (2.6) and (2.8) for our final results will be discussed below.

With these two assumptions Eqs. (2.7) and (2.2) can be rewritten as

$$\begin{aligned} \tilde{V}_T &= \frac{\rho_f \mathcal{V}}{k_B T^2 M m} \lim_{s \rightarrow 0^+} \\ &\times \int d\tilde{\mathbf{p}}^{\mathcal{N}} \prod_j \phi_j(p_j) \tilde{\mathbf{P}}_B(\vec{0} | G(s) | \vec{0}) \\ &\times \left[\frac{\tilde{\mathbf{p}}_2^2}{2m} - \frac{5}{2} k_B T \right] \frac{\tilde{\mathbf{p}}_2}{m} \end{aligned} \quad (2.9)$$

and

$$\begin{aligned} \xi^{-1} &= \frac{1}{M^2 k_B T} \lim_{s \rightarrow 0^+} \\ &\times \int d\tilde{\mathbf{p}}^{\mathcal{N}} \prod_j \phi_j(p_j) \tilde{\mathbf{P}}_B(\vec{0} | G(s) | \vec{0}) \tilde{\mathbf{P}}_B, \end{aligned} \quad (2.10)$$

where

$$G(s) \equiv \frac{1}{s + iL}, \quad (2.11)$$

L is the Liouville operator, and the matrix element for an operator O is defined as

$$(\vec{\mathbf{k}}^{\mathcal{N}} | O | \vec{\mathbf{k}}^{\mathcal{N}}) \equiv \frac{1}{\mathcal{V}^{\mathcal{N}}} \int d\tilde{\mathbf{r}}^{\mathcal{N}} e^{i\vec{\mathbf{k}}^{\mathcal{N}} \cdot \tilde{\mathbf{r}}^{\mathcal{N}}} O e^{i\vec{\mathbf{k}}^{\mathcal{N}} \cdot \tilde{\mathbf{r}}^{\mathcal{N}}}. \quad (2.12)$$

Note that in general, the "matrix" elements defined by Eq. (2.12) are still operators in momentum space. Equations (2.9) and (2.10) are useless in the absence

of a theory for the propagator $G(s)$. Such a theory exists and is presented in the next section.

III. KINETIC THEORY: GENERAL CONSIDERATIONS

The time-correlation functions appearing in Eqs. (2.9) and (2.10) (or their Laplace transforms) can be computed using the binary collision expansion.⁹ This method has been used previously in the calculation of the friction coefficient. To leading order in the density of the host gas, Zwanzig¹⁰ has shown the equivalence of this approach and that of the Boltzmann equation in the case of self-diffusion. Subsequently, much work has gone into the calculation of the density expansions of the other transport coefficients.¹¹ Unfortunately, the method is not valid at higher densities due to nonanalytic terms (i.e., $\rho^2 \ln \rho$) resulting from a special class of many-body collisions, the ring collisions¹² (see also below). These collisions are ultimately responsible for introducing hydrodynamic phenomena into kinetic theory. Examples are long-time tails¹³ and correlation anomalies in nonequilibrium systems.¹⁴ They can also be used to follow the transition of physical quantities from their low-density forms to their hydrodynamic values. Specifically, the transition of the friction constant from the value predicted by the Boltzmann equation to its Stokes value has been studied. For completeness, certain aspects of the calculation of the friction constant [Eq. (2.10)] will be repeated in this work.

The starting point of the calculation is the binary collision expansion for the propagator¹⁰:

$$\begin{aligned} G(s) &= G_0(s) - \sum_{\alpha} G_0(s) T_{\alpha}(s) G_0(s) \\ &+ \sum'_{\alpha, \beta} G_0(s) T_{\alpha}(s) G_0(s) T_{\beta}(s) G_0(s) + \dots, \end{aligned} \quad (3.1)$$

where G_0 is the free streaming propagator, T is the binary collision operator, α and β denote pairs of particles (including the B particle) and where \sum' implies that $\alpha \neq \beta$, etc.

A number of important properties [Eqs. (3.2)–(3.7)] of these operators are needed¹⁰.

$$(\vec{\mathbf{k}}^{\mathcal{N}} | G_0(s) | \vec{\mathbf{k}}^{\mathcal{N}}) = (s + i\vec{\mathbf{k}}^{\mathcal{N}} \cdot \vec{\mathbf{V}}^{\mathcal{N}})^{-1} \Delta(\vec{\mathbf{k}}^{\mathcal{N}} - \vec{\mathbf{k}}^{\mathcal{N}}), \quad (3.2)$$

where Δ is a Kronecker δ function and where $\vec{V}^{\mathcal{N}}$ is a vector whose elements are the particle velocities,

$$\begin{aligned} (\vec{k}^{\mathcal{N}} | T_{12}(s) | \vec{k}'^{\mathcal{N}}) \\ \propto \Delta(\vec{k}^{\mathcal{N}-2} - \vec{k}'^{\mathcal{N}-2}) \Delta(\vec{k}_1 + \vec{k}_2 - \vec{k}'_1 - \vec{k}'_2), \end{aligned} \quad (3.3)$$

$$(k^{\mathcal{N}} | T_{12} | k'^{\mathcal{N}}) \propto \mathcal{V}^{-1} \quad (3.4)$$

for a large system, and

$$\mathcal{L}_B = - \lim_{s \rightarrow 0^+} \int d\vec{p}_3 \phi_3(p_3) (\vec{0} | \mathcal{V} T_{B3} | \vec{0}), \quad (3.5)$$

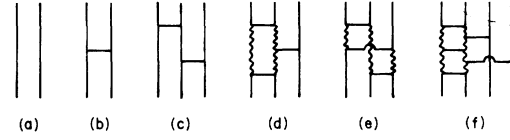


FIG. 1. Diagrammatic representation of some terms in the binary collision expansion of the Soret coefficient. Diagram (a) is free streaming, (b) a single collision, (c) a factorizable diagram, (d) a single nonexchange ring, (e) an exchange ring, and (f) a repeated ring. In all cases, the leftmost line corresponds to the B particle.

where \mathcal{L}_B is the Boltzmann-Lorentz collision operator. When \mathcal{L}_B acts on any function of \vec{p}_B , we obtain

$$\mathcal{L}_B f(\vec{p}_B) = - \int d\vec{p}_3 \phi_3(\vec{p}_3) \int_0^\infty b db \int_0^{2\pi} d\psi | \vec{V}_B - \vec{V}_3 | [f(\vec{p}_B) - f(\vec{p}_B^*)], \quad (3.6)$$

where b is the impact parameter, ψ is the azimuthal angle, and $*$ denotes the value of \vec{p}_B before the collision which results in final momenta \vec{p}_B and \vec{p}_3 .

The linearized Boltzmann collision operator for the gas particle \mathcal{L}_F is related to T by

$$\mathcal{L}_F = - \lim_{s \rightarrow 0^+} \int d\vec{p}_3 \phi_3(p_3) (\vec{0} | \mathcal{V} T_{23} | \vec{0}) (1 + \mathcal{P}_{23}), \quad (3.7)$$

where \mathcal{P}_{23} is the particle exchange operator which exchanges the labels on gas particles 2 and 3. The derivation of Eqs. (3.2)–(3.7) is straightforward and the reader is referred to Zwanzig¹⁰ for details.

By inserting Eq. (3.1) into (2.8) a “naive” density expansion for \vec{V}_T is obtained:

$$\begin{aligned} \vec{V}_T = \frac{\rho_F}{mMk_B T^2} \lim_{s \rightarrow 0^+} \int d\vec{p}^{\mathcal{N}} \prod_j \phi_j(p_j) \vec{P}_B \left[-\frac{1}{s^2} (\vec{0} | \mathcal{V} T_{B2} | \vec{0}) + \frac{n_f}{s^3} (\vec{0} | \mathcal{V} T_{B2} | \vec{0}) (\vec{0} | \mathcal{V} T_{23} | \vec{0}) \right. \\ \left. + \frac{n_f}{s^3} (\vec{0} | \mathcal{V} T_{B3} | \vec{0}) (\vec{0} | \mathcal{V} T_{23} | \vec{0}) \right. \\ \left. + \frac{n_f}{s^3} (\vec{0} | \mathcal{V} T_{B3} | \vec{0}) (\vec{0} | \mathcal{V} T_{B2} | \vec{0}) + \dots \right] \frac{\vec{p}_2}{m} \left[\frac{p_2^2}{2m} - \frac{5}{2} k_B T \right], \end{aligned} \quad (3.8)$$

where n_f is the gas number density and where the wave-number conservation rules [cf. Eqs. (3.2) and (3.3)] have been used. In addition, we have used the fact that the first T operator must involve the B particle and the last must involve particle 2 in obtaining Eq. (3.8) (see, e.g., Ref. 10 for a discussion of this point). Equation (3.8) contains all terms involving up to two T operators. The expansion is termed naive since each term diverges as $s \rightarrow 0$. The common approach is to resum the most (or next most) divergent terms in s at each order of n_f . This direct resummation procedure is most easily understood by using a graphical notation, introduced by Bartis and Oppenheim.¹⁵ Roughly speaking, the different diagrams represent different types of collisions. For example, in Fig. 1(c), B collides with particle 2 which had collided with a third particle at some earlier time. In Fig. 1(e), B collides with 2 after colliding with 3, after 2 and 3 collided.

In Fig. 1 some of the terms appearing in Eq. (3.8) as well as some of the higher-order ones are depicted. The graphs should be read from top to bottom. Each particle has a vertical line corresponding to free propagation. The horizontal lines imply T operators involving the connected particles (notice that the first T involves B and the last one 2). The wiggly vertical lines denote summation over an intermediate wave vector. For example, the contribution of Fig. 1(d) to $(\vec{0} | G(s) | \vec{0})$ is

$$\begin{aligned}
& -\frac{n_f}{s^2} \int \frac{d\vec{k}}{(2\pi)^3} (\vec{0} | \mathcal{V} T_{B2} | \vec{k}, -\vec{k}) \frac{1}{s + i\vec{k} \cdot (\vec{V}_B - \vec{V}_2)} (\vec{k}, -\vec{k} | \mathcal{V} T_{23} | \vec{k}, -\vec{k}) \\
& \quad \times \frac{1}{s + i\vec{k} \cdot (\vec{V}_B - \vec{V}_2)} (\vec{k}, -\vec{k} | \mathcal{V} T_{B2} | \vec{0}) . \tag{3.9}
\end{aligned}$$

In general, the sign of a given diagram is $(-1)^\sigma$, where σ is the number of T 's, the power of the density is given by the number of different gas particles (other than particle 2) taking part in the event, and the power of s^{-1} is equal to the minimum number of horizontal strips not containing any intermediate wave vectors. The intermediate wave-vector sums protect the divergence in s^{-1} . This protection is not complete, a $\ln(s)$ divergence still remaining.^{3(b),12,13,16} [Strictly speaking, this is true in two dimensions (2D). For three dimensions (3D) the $\ln(s)$ divergence occurs with a four-body collision.]

Clearly, at a given order in density, the most divergent diagrams are those containing *no* intermediate wave vectors. These are known as the factorizable diagrams.¹⁵ At low enough density, it is sufficient to resum just these diagrams. The result is

$$\begin{aligned}
\tilde{V}_T = & \frac{\rho_F}{mMk_B T^2} \lim_{s \rightarrow 0^+} \int d\vec{P}_B d\vec{p}_2 \phi_B(P_B) \phi_2(p_2) \vec{P}_B \frac{1}{(s - n_f \mathcal{L}_B)} (\vec{0} | \mathcal{V} T_{B2} | \vec{0}) \\
& \times \frac{1}{(s - n_f \mathcal{L}_F)} \frac{\vec{p}_2}{m} \left[\frac{p_2^2}{2m} - \frac{5}{2} k_B T \right] . \tag{3.10}
\end{aligned}$$

In obtaining Eq. (3.10), the equivalence of the gas particles has been used. As we shall see, Eq. (3.10) is equivalent to the results of the Boltzmann equation. No effects of correlated many-body collisions are included.

The diagrams containing single intermediate wave-vector sums are known as ring diagrams. They are the next most divergent terms in s at a given order in density. We distinguish between two types of ring diagrams containing the B particle. The nonexchange type, which begins and ends with a T involving the B particle, and the exchange type which contains an intermediate T after which B no longer appears. For example, Fig. 1(d) is a nonexchange ring collision and Fig. 1(e) is an exchange one. Closed-form expressions can be obtained for the sums of all these ring collisions in the following way. Note (cf. Kawasaki and Oppenheim¹² for more details) that any of the nex (nonexchange ring) diagrams can be written in the form

$$\frac{(-n_f)^n}{s^2} (\vec{0} | \mathcal{V} T_{B2} \Lambda_{\alpha_1}(i_1) \cdots \Lambda_{\alpha_n}(i_n) \mathcal{V} G_0 T_{B2} | \vec{0}) , \tag{3.11}$$

where $i_j = B$ or 2 (2 need not be the special gas particle here) and

$$\alpha_j = \begin{cases} l, & i_j = B \\ l \text{ or } d, & i_j = 2 . \end{cases}$$

The so-called "loop" and "dot" operators are defined as¹²

$$\Lambda_l(i) \equiv \int d\vec{p}_3 \phi(p_3) G_0 \mathcal{V} T_{i3} , \tag{3.12}$$

and

$$\Lambda_d(2) \equiv \int d\vec{p}_3 \phi(p_3) G_0 \mathcal{V} T_{23} \mathcal{P}_{23} . \tag{3.13}$$

Summing over n , $\{\alpha_j\}$ and $\{i_j\}$ gives

$$\begin{aligned}
R_{\text{nex}} = & \frac{1}{s^2} \left[\vec{0} | \mathcal{V} T_{B2} \right. \\
& \times \frac{1}{1 + n_f [\Lambda_l(2) + \Lambda_d(2) + \Lambda_l(B)]} \\
& \left. \times \mathcal{V} G_0 T_{B2} | \vec{0} \right] , \tag{3.14}
\end{aligned}$$

where we have also used the fact that³

$$(\vec{0} | \mathcal{V} T_{B2} G_0 \mathcal{V} T_{B2} | \vec{0}) = 0 , \tag{3.15}$$

since particles B and 2 can collide only once without the intervention of a third particle.

In an analogous manner, the exchange rings sum up to yield

$$\begin{aligned}
R_{\text{ex}}(B,2) = & -\frac{n_f}{s^2} \int d\vec{p}_3 \phi_3(p_3) \left(\vec{0} \left| \mathcal{Y} T_{B2} \frac{1}{1+n_f[\Lambda_l(2)+\Lambda_d(2)+\Lambda_l(B)]} \right. \right. \\
& \times G_0 \mathcal{Y} T_{B3} \frac{1}{1+n_f[\Lambda_l(2)+\Lambda_d(2)+\Lambda_l(3)+\Lambda_d(3)]} \\
& \left. \left. \times G_0 \mathcal{Y} T_{23}(1+\mathcal{P}_{23}) \right| \vec{0} \right). \tag{3.16}
\end{aligned}$$

The single ring sums no longer diverge like $(1/s^2)\ln s$. In the standard applications of kinetic theory (i.e., to molecular systems) they result in logarithmic terms in the density expansion of the transport coefficients. As we now show they also diverge when $R/l \rightarrow \infty$. It is for this reason that they are kept here. Moreover, since it is just this dependence which is under investigation, we omit all ring diagrams which do not include the B particle (i.e., the host gas is dilute enough). That the ring divergence is eliminated can be seen in the following way: Recall that a typical ring contribution could be written as [see, e.g., Eq. (3.9)]

$$\begin{aligned}
& \frac{n_f}{s^2} \int d\vec{k} (\vec{0} | VT_{B2} | \vec{0}) \frac{1}{s+i\vec{k}\cdot\vec{v}_{B2}} \\
& \times (\vec{0} | VT_{23} | \vec{0}) \frac{1}{s+i\vec{k}\cdot\vec{v}_{B2}} (\vec{0} | VT_{B2} | \vec{0}),
\end{aligned}$$

where the k dependence of the T 's is omitted. Treating the T matrix elements as constants, shows that in 2D, a logarithmic infrared divergence sets in as $s \rightarrow 0$, i.e., the contribution is $O(s^{-2}\ln s)$. In 3D this occurs with a four-body collision.

The ring resummation replaces the free propagators by effective ones—namely, propagation with Boltzmann collisions with the other bath particles. These extra collisions provide additional damping and eliminate the divergence. To see this, we note that the dominant contributions to the small- k parts

of the integrals is [cf. Eq. (3.14) and below]

$$\int_{k < k_c} d\vec{k} (\vec{0} | VT_{B2} | \vec{0}) \frac{1}{s+\Gamma k^2},$$

where we have again ignored the operator character of the T 's (this is corrected below) and inserted the propagator appropriate for a hydrodynamic part of the spectrum (e.g., a shear mode). The constant Γ is of the order of the bath kinematic viscosity or $O(l)$. Finally, the size dependence of T_{B2} is $O(R^2)$. Thus, the magnitude of the above integral is $O(k_c R^2/l)$ in 3D. The cutoff accounts for our neglect of the k dependence of T_{B2} and for the use of the hydrodynamic approximation (see below). It is $O(R^{-1})$ for $R \gg l$ or $O(l^{-1})$ for $R \ll l$. In the former case, we thus find that the integral in question is $O(R/l)$, which diverges when $R \rightarrow \infty$. Since this integral is essentially the ring correction factor to T_{B2} [see Eq. (3.14)], we see that for $R \gg l$, more than single rings must be kept. Physically, what is happening is as follows: After colliding with B a gas particle travels a distance $O(l)$ where it encounters another gas particle. If $l/R \gg 1$, the solid angle subtended by B at this collision site is very small. On the other hand, for large enough R , $l/R \ll 1$, the B particle looks like an infinite plane and the probability of recollision is close to unity. The divergence of the nonexchange ring diagrams is thus further renormalized by repeated rings.^{4(d)} Formally, this gives

$$\begin{aligned}
R_{RR}(B,2) = & +\frac{1}{s^2} (\vec{0} | VT_{B2} \mathcal{G}_{B2} VT_{B2} - VT_{B2} \mathcal{G}_{B2} VT_{B2} \mathcal{G}_{B2} VT_{B2} + \cdots | \vec{0}) \\
= & -\frac{1}{s^2} \left(\vec{0} \left| \left[\frac{1}{1+\mathcal{Y} T_{B2} \mathcal{G}_{B2}} - 1 \right] \mathcal{Y} T_{B2} \right| \vec{0} \right), \tag{3.17}
\end{aligned}$$

where

$$\begin{aligned}
\mathcal{G}_{B2} \equiv & \{1+n_f[\Lambda_l(2)+\Lambda_d(2)+\Lambda_l(B)]\}^{-1} G_0 \\
= & \left[G_0^{-1} + n_f \mathcal{Y} \int d\vec{p}_3 \phi(p_3) [T_{B3} + T_{23}(1+\mathcal{P}_{23})] \right]^{-1}. \tag{3.18}
\end{aligned}$$

The second equality in Eq. (3.17) follows when we recognize the repeated-ring series as a geometric series. Notice that there is still a s^{-2} divergence, which merely signals the fact that factorizable diagrams must be summed. The second equality in Eq. (3.18) follows from Eqs. (3.12) and (3.13). R_{RR} is referred to as the repeated-ring operator. The quantity \mathcal{G}_{B2} is a propagator for the $(B,2)$ pair of particles each undergoing uncorrelated binary collisions with the gas. Similarly, R_{ex} is modified by repeated nonexchange rings.

The general diagram will be composed of factorizable parts, nonexchange rings and repeated rings, involving B and some fluid particle (not 2) and either of T_{B2} , an exchange or nonexchange ring involving 2. As was the case above, this generates yet another geometric series. The resummation is now straightforward and we obtain

$$\begin{aligned} \tilde{V}_T = & -\frac{\rho_F}{mMk_B T^2} \lim_{s \rightarrow 0^+} \int d\vec{P}_B d\vec{p}_2 \phi_B(P_B) \phi_2(\vec{p}_2) \vec{P}_B \mathcal{G}_B^{(1)}(s) \\ & \times \left[\left[\vec{0} \left| \frac{1}{1 + \mathcal{V}T_{B2} \mathcal{G}_{B2}} \mathcal{V}T_{B2} \left(1 + n_f \mathcal{G}_{B2} \int d\vec{p}_3 \phi_3(p_3) \mathcal{V}T_{B3} \mathcal{G}_{23} \mathcal{V}T_{23} (1 + \mathcal{P}_{23}) \right) \right| \vec{0} \right] \right] \\ & \cdot \frac{1}{s - n_f \mathcal{L}_F} \frac{\vec{p}_2}{m} \left[\left[\frac{p_2^2}{2m} - \frac{5}{2} k_B T \right] \right], \end{aligned} \quad (3.19)$$

where the one-particle B propagator is defined by

$$\mathcal{G}_B^{(1)}(s) \equiv \left[s + n_f \int d\vec{p}_3 \phi_3(p_3) \left[\vec{0} \left| \frac{1}{1 + \mathcal{V}T_{B3} \mathcal{G}_{B3}} \mathcal{V}T_{B3} \right| \vec{0} \right] \right]^{-1}, \quad (3.20a)$$

$$\mathcal{G}_{23} = \left[G_0^{-1} + n_f \int d\vec{p}_4 \phi_4(p_4) [\mathcal{V}T_{24} (1 + \mathcal{P}_{24}) + \mathcal{V}T_{34} (1 + \mathcal{P}_{34})] \right]^{-1}, \quad (3.20b)$$

Eq. (3.5) having been used. Equation (3.19) is most easily proved by expanding the propagators defined by Eqs. (3.20a) and (3.20b) back into the binary collision expansion, keeping the parts due to repeated rings together [cf. Eq. (3.17)]. This form for \tilde{V}_T will be referred to as the repeated-ring approximation for \tilde{V}_T . Notice the similarity between Eqs. (3.19), (3.20), and Eq. (3.10).

The inclusion of the ring collisions has renormalized the Boltzmann propagators as well as the $(B,2)$ scattering operator (this plays the role of the mode-coupling vertex). No renormalization of the fluid propagator appears since gas-gas rings have been omitted.

The ring—repeated-ring resummation results presented here differ slightly from the standard ones. If the technique is applied to the friction constant, one obtains

$$\xi^{-1} \equiv \frac{\lim_{s \rightarrow 0^+}}{M^2 k_B T} \int d\vec{P}_B \phi_B(\vec{P}_B) \vec{P}_B \mathcal{G}_B^{(1)}(s) \vec{P}_B, \quad (3.21)$$

this being the well-known result.⁴

The main results of this section are Eqs. (3.19)–(3.21). A number of approximations have been made: Only single rings have been included.

No fluid renormalization has been considered. As was discussed above, this is not a full density expansion and we have kept only those terms which are important for the Boltzmann behavior or for a large B particle [i.e., we neglect terms $O(\sigma/R)$ at higher densities, σ being the “diameter” of the host-gas particles].

IV. HYDRODYNAMIC APPROXIMATION

As was mentioned earlier, the repeated-ring approximation has been used in many applications, including self-diffusion,^{4(c),4(d)} diffusion in a Lorentz gas,¹⁷ and in the calculation of the friction coefficient.⁵ The most common approach used in carrying out these calculations is known as the hydrodynamic approximation (see, however, Ref. 18). In short, this approximation takes a spectral representation for the one- and two-body propagators contained in Eqs. (3.19)–(3.21) and retains only those terms corresponding to the densities of the conserved variables. The motivation for this is the fact that these terms are responsible for the anomalous time dependence (i.e., $\ln s$) which required the ring resummations in the first place. The other terms give a contribution $O(\rho \ln \rho)$ or $O(R \ln R)$ and are

less important (see below). The calculation of ξ is somewhat simpler than \tilde{V}_T and we consider it first.

A. Friction constant ξ

The friction constant ξ has been studied within the context of the repeated-ring approximation.⁵ The analysis, albeit quite complicated if carried out

$$\mathcal{G}_B(s) = \left[s + n_f \int d\vec{p}_3 \phi(\vec{p}_3) \frac{1}{1 + (\vec{0} | \mathcal{V} T_{B3} | \vec{0}) \int_{k < k_c} \frac{d\vec{k}}{(2\pi)^3} \frac{1}{s + i\vec{k} \cdot (\vec{V}_B - \vec{V}_3) - n_f [\mathcal{L}_B - \mathcal{L}_f(3)]}} \right]^{-1} \times (\vec{0} | \mathcal{V} T_{B3} | \vec{0}) \quad (4.1)$$

where $k_c \sim O(R^{-1})$. The integrand of the k integral in Eq. (4.1) is the Boltzmann propagator for the B and gas particle (3). It describes the propagation of the pair, as influenced by multiple uncorrelated binary collisions with other gas particles. How important are the various parts of this propagator? Clearly,

$$V_B \sim \sqrt{k_B T / M} \ll \sqrt{k_B T / m} \sim V_3 \quad (4.2a)$$

since $(m/M) \ll 1$. Moreover, since \mathcal{L}_B and \mathcal{L}_f are Boltzmann-Lorentz and Boltzmann collision operators, it is easy to see that

$$\mathcal{L}_B \sim R^2 \frac{m}{M} \left[\frac{k_B T}{m} \right]^{1/2} \ll \sigma^2 \left[\frac{k_B T}{m} \right]^{1/2} \sim \mathcal{L}_f. \quad (4.2b)$$

Of course, these are operators, and hence Eqs. (4.2a) and (4.2b) must be treated with some care. Nonetheless, for the present case, we can neglect the parts of \mathcal{G}_B which pertain to B .

The right eigenfunctions ψ of the gas Boltzmann equation satisfy

$$[-i\vec{k} \cdot \vec{V}_3 - n_f \mathcal{L}_f(3)] \psi_{\alpha, \vec{k}}(\vec{p}_3) \equiv \lambda_{\alpha}(\vec{k}) \psi_{\alpha, \vec{k}}(\vec{p}_3). \quad (4.3)$$

For a reasonable choice of the potential,^{3(c)} the eigenfunctions are complete and there are five eigenfunctions ($\alpha = 1, \dots, 5$) whose eigenvalues vanish in the limit $k \rightarrow 0$. These are the hydrodynamic eigenvectors. The left eigenfunctions are related to the right ones through complex conjugation.^{3(c)} This implies that the eigenfunctions can be chosen

rigorously, yields a rather simple expression for the size dependence of ξ . Here, we present a cruder version of the more general argument (see Ref. 5 for more details), which is sufficient for our purposes.

In the wave-vector representation, for k 's smaller than the inverse range of the interaction (i.e., R^{-1}), the k dependence of the T -matrix elements can be neglected. In this case $\mathcal{G}_B^{(1)}$ can be written as [cf. Eqs. (3.20) and (3.18)]

such that

$$\langle \bar{\psi}_{\alpha_1} | \psi_{\alpha_2} \rangle \equiv \int d\vec{p}_3 \phi_3(p_3) \psi_{\alpha_1, \vec{k}}(\vec{p}_3) \psi_{\alpha_2, \vec{k}}(\vec{p}_3) = \delta_{\alpha_1, \alpha_2}, \quad (4.4)$$

where the overbar denotes complex conjugation and where the customary inner product $\langle | \rangle$ for kinetic theory has been introduced.

Using Eqs. (4.2a) and (4.2b), we see that the ratio of the convective term to that containing the collision operator on the left-hand side (lhs) of Eq. (4.3) is $O(kl)$ [$l \sim (n_f \sigma^2)^{-1}$ is the mean free path]. For small enough k we can thus treat the convective term as a perturbation [this will force us to take $k_c \sim \min(l^{-1}, R^{-1})$]. In this case we will use the eigenfunction in the limit $k \rightarrow 0$ denoted by $\psi_{\alpha}^{(0)}$ and expand the eigenvalues in a power series in (kl) . The manipulations are standard, and the reader is referred to Refs. 14, 3(b), or 5(b) for details.

Consider what happens when $(\vec{0} | \mathcal{V} T_{B3} | \vec{0})$ acts on a function $f(\vec{p}_3, \vec{p}_B)$:

$$\begin{aligned} (\vec{0} | \mathcal{V} T_{B3} | \vec{0}) f &= \int_0^{\infty} b db \int_0^{2\pi} d\psi | \vec{V}_B - \vec{V}_3 | \\ &\quad \times [f(\vec{P}_B, \vec{p}_3) - f(\vec{P}_B^*, \vec{p}_3^*)]. \end{aligned} \quad (4.5)$$

For a large enough mass ratio, the change in \vec{P}_B is $O(\sqrt{m/M})$ and thus

$$\begin{aligned}
& (\vec{0} | \mathcal{V} T_{B,3} | \vec{0}) f \\
& \sim \int_0^\infty b db \int_0^{2\pi} d\psi | \vec{V}_B - \vec{V}_3 | \\
& \quad \times [f(\vec{P}_B, \vec{p}_3) - f(\vec{P}_B, \vec{p}_3^*)] \\
& + O(\sqrt{m/M}). \tag{4.6}
\end{aligned}$$

Thus $(\vec{0} | \mathcal{V} T_{B,3} | \vec{0})$ does not act on \vec{P}_B in a composite function of \vec{P}_B and \vec{p}_3 (assuming the leading order result is nonvanishing). Using Eqs. (4.3), (4.4), and (4.6) in (4.1) allows us to rewrite the one-particle B propagator as

$$\begin{aligned}
\mathcal{G}_B^{(1)}(s) = & \left[s - n_f \left[\mathcal{L}_B + \int d\vec{p}_3 \phi_3(\vec{p}_3) (\vec{0} | \mathcal{V} T_{B,3} | \vec{0}) \psi_{\alpha_1}^{(0)}(\vec{p}_3) \right. \right. \\
& \left. \left. \times \left[\frac{1}{\underline{Q} + \underline{\mathcal{I}}} \right]_{\alpha_1 \alpha_2} \int d\vec{p}_4 \phi_4(\vec{p}_4) \psi_{\alpha_2}^{(0)}(\vec{p}_4) (\vec{0} | \mathcal{V} T_{B,4} | \vec{0}) \right] \right]^{-1}, \tag{4.7}
\end{aligned}$$

where

$$\mathcal{Q}_{\alpha_1, \alpha_2} \equiv \delta_{\alpha_1, \alpha_2} \left[\int_{k \leq k_c} \frac{d\vec{k}}{(2\pi)^3} \frac{1}{s + \lambda_\alpha(k)} \Lambda_\alpha(\hat{k}) \right]^{-1}, \tag{4.8}$$

$$\tau_{\alpha_1, \alpha_2} \equiv \int d\vec{p}_3 \phi(\vec{p}_3) \psi_{\alpha_1}^{(0)}(\vec{p}_3) (\vec{0} | \mathcal{V} T_{B,3} | \vec{0}) \psi_{\alpha_2}^{(0)}(\vec{p}_3) |_{\vec{P}_B=0}. \tag{4.9}$$

The quantity $\Lambda_\alpha(\hat{k})$ (\hat{k} denotes a unit vector) accounts for any directional dependence of $\psi_\alpha^{(0)}$ on k . In the hydrodynamic approximation only those terms for which $\alpha_1, \alpha_2 = 1, \dots, 5$ are kept.

The most important contributions come from those eigenfunctions whose eigenvalues are real [and hence $O(k^2)$ in the hydrodynamic approximation]. For the case at hand, these correspond to the heat and shear modes. That is,

$$\psi_{\text{shear}}^{(0)}(\vec{p}_3) = (1 - \hat{k} \hat{k}) \cdot \vec{p}_3 / (mk_B T)^{1/2}, \quad \mathcal{Q}_{\text{shear}} = \left[\frac{k_c}{3\pi^2 \nu} \right]^{-1}, \tag{4.10a}$$

and

$$\psi_{\text{heat}}^{(0)}(\vec{p}_3) = \sqrt{2/5} \frac{1}{k_B T} \left[\frac{p_3^2}{2m} - \frac{5}{2} k_B T \right], \quad \mathcal{Q}_{\text{heat}} = \left[\frac{k_c}{3\pi^2 \Gamma_T} \right]^{-1}, \tag{4.10b}$$

where ν is the kinematic viscosity of the host gas and Γ_T is its thermal-diffusion constant, both are $O(n_f^{-1})$. Neglecting all other modes, and assuming that the B particle is spherical, implies that $\underline{\mathcal{I}}$ is diagonal. Hence

$$\begin{aligned}
\mathcal{G}_B^{(1)}(s) \approx & \left[s - n_f \mathcal{L}_B - n_f \int d\vec{p}_3 \phi_3(p_3) (\vec{0} | \mathcal{V} T_{B,3} | \vec{0}) \right. \\
& \times \left[\frac{\vec{p}_3 \int d\vec{p}_4 \phi_4(p_4) \vec{p}_4 (\vec{0} | \mathcal{V} T_{B,4} | \vec{0})}{(3\pi^2 \nu / k_c + \tau_{\text{shear}}) m k_B T} + \frac{2}{5(k_B T)^2} \left[\frac{p_3^2}{2m} - \frac{5}{2} k_B T \right] \right. \\
& \left. \left. \times \int d\vec{p}_4 \phi(p_4) \left[\frac{p_4^2}{2m} - \frac{5}{2} k_B T \right] (\vec{0} | \mathcal{V} T_{B,4} | \vec{0}) \right] \right]^{-1} \tag{4.11}
\end{aligned}$$

The one-particle propagator is still an operator. In order to compute ξ^{-1} [cf. Eq. (3.21)] its inverse must be found. A common technique used in solving the integral equation which defines the inverse in Eq. (4.11) is to perform a basis-set expansion, the basis functions usually being taken to be the Sonine³ polynomials. The B -particle's momentum is one of the Sonine polynomials. Thus in the first approximation [cf. Eqs. (4.11) and (3.21)]

$$\begin{aligned}
\xi = & - \left[n_f \int \frac{d\vec{P}_B \phi_B(P_B) \vec{P}_B}{k_B T} \left\{ \mathcal{L}_B \vec{P}_B + \int d\vec{p}_3 \phi_3(p_3) (\vec{0} | \mathcal{V} T_{B3} | \vec{0}) \right. \right. \\
& \times \left[\frac{\vec{p}_3}{mk_B T} \int \frac{d\vec{p}_4 \phi(p_4) \vec{p}_4 (\vec{0} | \mathcal{V} T_{B4} | \vec{0}) \vec{P}_B}{(3\pi^2 \nu / k_c + \tau_{\text{shear}})} \right. \\
& + \frac{2}{5k_B T^2} \frac{(p_3^2/2m - 5/2k_B T)}{(3\pi^2 \Gamma_T / k_c + \tau_{\text{heat}})} \\
& \left. \left. \times \int d\vec{p}_4 \phi(p_4) \left[\frac{p_4^2}{2m} - \frac{5}{2} k_B T \right] (\vec{0} | \mathcal{V} T_{B4} | \vec{0}) \vec{P}_B \right] \right\} \right]. \tag{4.12}
\end{aligned}$$

Since $\vec{P}_B + \vec{p}_i$ is conserved in a (B, i) collision, one can replace \vec{P}_B by $-\vec{p}_4$ in the last term in Eq. (4.12). This yields a factor $\tau_{\text{heat, shear}}$ which we have already neglected. The remaining terms can be rewritten as

$$\begin{aligned}
\xi = & + n_f m \tau_{\text{shear}} - n_f m \frac{\tau_{\text{shear}}^2}{3\pi^2 \nu / k_c + \tau_{\text{shear}}} \\
= & n_f m \frac{\tau_{\text{shear}}}{[1 + \tau_{\text{shear}} k_c / (3\pi^2 \nu)]}. \tag{4.13}
\end{aligned}$$

At very low density the Boltzmann result (in the one Sonine polynomial approximation) is recovered, i.e.,

$$\xi \rightarrow \xi_B = n_f m \tau_{\text{shear}}, \tag{4.14}$$

while at high density

$$\xi \rightarrow \frac{3\pi^2 \eta}{k_c}. \tag{4.15}$$

(η is the shear viscosity.) For $k_c \sim O(2\pi/R)$ this is the hydrodynamic result,¹⁹ ignoring for the moment the question of slip or stick prefactor. In order to remove k_c completely, the small- k approximation used for the T -matrix elements must be eliminated and details of the scattering event, on the scale of the interaction, must be considered. This has been done⁵ although for our purpose we can treat k_c as

an adjustable parameter to be determined in a separate measurement of the B -particle diffusion constant, friction constant, momentum relaxation time, etc. In summary, then

$$\xi = \frac{\xi_B}{1 + \xi_B k_c / (3\pi^2 \eta)}. \tag{4.16}$$

Notice that for $l \gg R$, $k_c \sim l^{-1}$ and thus the ring-repeated-ring corrections are $O(n_f^2)$.

B. Thermophoretic velocity \vec{V}_T

The calculation of \vec{V}_T follows that for ξ in principle, although it is somewhat more complicated. The expression for \vec{V}_T [cf. Eq. (3.19)] splits into two parts, the part containing the “exchange rings” (i.e., R_{ex}) and the rest. In Appendix A we show that the contribution from the exchange collisions is negligible.

The remaining part of \vec{V}_T is made up of three factors: the single-particle propagator $\mathcal{G}_B^{(1)}(s)$, the $(B, 2)$ repeated-ring propagator, and the gas-linearized Boltzmann propagator. As in the Sec. IV A, we will use a one-Sonine polynomial approximation for $\mathcal{G}_B^{(1)}(s)$ as well as for $(s - n_f \mathcal{L}_f)^{-1}$. Noting that $\vec{p}_2/m [p_2^2/2m - (5/2)k_B T]$ is a Sonine polynomial and using the results of the preceding section allows us to write

$$\vec{V}_T = \frac{-\rho F}{mk_B T^2} \lim_{s \rightarrow 0^+} \xi^{-1} \int d\vec{P}_B d\vec{p}_2 \phi_B(\vec{P}_B) \phi_2(p_2) \vec{P}_B \left[\left[\vec{0} \left| \frac{1}{1 + T_{B2} \mathcal{G}_{B,2}} \mathcal{V} T_{B2} \right| \vec{0} \right] \frac{\vec{p}_2}{2m} \left[\frac{p_2^2}{2m} - \frac{5}{2} k_B T \right] \right] \frac{\lambda m}{\frac{5}{2} k_B^2 T n_f}, \tag{4.17}$$

where we have used Eq. (3.21) and have introduced the translational part of the gas thermal conductivity λ , given in the one Sonine polynomial approximation by³

$$\lambda^{-1} = \left[\frac{-4m^2T}{25(k_B T)^5} \right] \int d\vec{p}_2 \phi_2(\vec{p}_2) \frac{\vec{p}_2}{m} \left[\frac{p_2^2}{2m} - \frac{5}{2} k_B T \right] \mathcal{L}_f \frac{\vec{p}_2}{m} \left[\frac{p_2^2}{2m} - \frac{5}{2} k_B T \right]. \quad (4.18)$$

Hence, in the single basis function expansion, all that remains to be done is to evaluate the repeated-ring contribution in Eq. (4.17). The way this is performed is exactly as was done in the calculation of ξ , that is to use the hydrodynamic approximation. The result is

$$\begin{aligned} \tilde{V}_T = & \frac{2m\lambda}{5(k_B T)^3 \xi} \left[\int d\vec{p}_2 \phi_2(\vec{p}_2) \vec{p}_2 \psi_\alpha^{(0)}(\vec{p}_2) \left[\frac{\underline{Q} \cdot 1}{(\underline{Q} + \underline{\tau})} \right]_{\alpha\beta} \right. \\ & \left. \times \int d\vec{p}_2 d\vec{P}_B \phi_B(\vec{P}_B) \phi_2(\vec{p}_2) \psi_B^{(0)}(\vec{p}_2) (\vec{0} | \mathcal{V} T_{B2} | \vec{0}) \frac{\vec{p}_2}{m} \left[\frac{p_2^2}{2m} - \frac{5}{2} k_B T \right] \right], \end{aligned} \quad (4.19)$$

where we have used Eqs. (4.8) and (4.9), and we have used the fact that $\vec{p}_2 + \vec{P}_B$ is conserved to replace \vec{P}_B by $-\vec{p}_2$ in Eq. (4.17). As before, only α, β corresponding to hydrodynamic modes are included. Of these, the shear contribution is most important, and hence,

$$\tilde{V}_T \approx \frac{2m\lambda}{5(k_B T)^3 \xi} \frac{3\pi^2\nu}{k_c \left[\frac{3\pi^2\nu}{k_c} + \tau_{\text{shear}} \right]} \int d\vec{p}_2 d\vec{P}_B \phi_2(p_2) \phi_B(\vec{P}_B) \vec{p}_2 (\vec{0} | \mathcal{V} T_{B2} | \vec{0}) \frac{\vec{p}_2}{m} \left[\frac{p_2^2}{2m} - \frac{5}{2} k_B T \right], \quad (4.20)$$

which follows from Eq. (4.10a). Using our result for ξ [cf. Eq. (4.13)] gives

$$\tilde{V}_T = \frac{2}{5} \frac{\lambda}{n_f (k_B T)^3 \tau_{\text{shear}}} \int d\vec{p}_2 d\vec{P}_B \phi_2(p_2) \phi_B(\vec{P}_B) \vec{p}_2 (\vec{0} | \mathcal{V} T_{B2} | \vec{0}) \frac{\vec{p}_2}{m} \left[\frac{p_2^2}{2m} - \frac{5}{2} k_B T \right]. \quad (4.21)$$

All dependence on k_c has dropped out. Moreover, Eq. (4.21) is exactly what would have been obtained had we started in the Boltzmann limit [i.e., Eq. (3.10)]. Thus, the effects of rings-repeated rings completely drop out of the thermophoretic velocity. The exact cancellation occurred largely due to the one Sonine polynomial and hydrodynamic approximations. However, it is possible that this cancellation is more general. The cancellation of the ring-repeated-ring corrections to \tilde{V}_T yields a result which is completely analogous to the mode-coupling result for the Soret coefficient (remember that the two are essentially the same). In that case (cf. Sec. III of I), the mode-coupling parts dropped out. In fact, technically the two theories have very similar structures, the main differences arising in the nature of the vertices and in the bare quantities. In any case, the full effect of rings will occur as a ratio of the ring-repeated-ring corrections for the friction, to those involved in \tilde{V}_T . This ratio should be $O(1)$.

C. Relationship to the $(B-2)$ scattering cross section and collision integrals

The manipulations leading to the expressions for ξ [cf. Eq. (4.13) or (4.16)] and \tilde{V}_T [cf. Eq. (4.21)] have, to a large extent, been independent of the choice of scattering law between the B and gas particles. The only way this dynamical information appeared was via

$$\tau_{\text{shear}} = \frac{1}{mk_B T} \int d\vec{p}_2 \phi_2(p_2) \vec{p}_2 (\vec{0} | \mathcal{V} T_{B2} | \vec{0}) \vec{p}_2 \quad (4.22)$$

and

$$\mathcal{J} \equiv \int d\vec{p}_2 \phi_2(p_2) \int d\vec{P}_B \phi_B(P_B) \vec{p}_2 (\vec{0} | \mathcal{V} T_{B2} | \vec{0}) \frac{\vec{p}_2}{m} \left[\frac{p_2^2}{2m} - \frac{5}{2} k_B T \right] \quad (4.23)$$

$$= \int d\vec{p}_2 d\vec{P}_B \phi_2(p_2) \phi_B(P_B) \frac{\vec{p}_2}{m} \left[\frac{p_2^2}{2m} - \frac{5}{2} k_B T \right] (\vec{0} | \mathcal{V} T_{B2} | \vec{0}) \vec{p}_2, \quad (4.24)$$

where the last equality follows from stationarity. When $M \gg m$, we can neglect the motion of B in the collision and thereby obtain

$$\mathcal{J} \approx \int d\vec{p}_2 \phi_2(p_2) \frac{\vec{p}_2}{m} \left[\frac{p_2^2}{2m} - \frac{5}{2} k_B T \right] (\vec{0} | \mathcal{V} T_{B2} | \vec{0}) \vec{p}_2 \Big|_{\vec{P}_B=0}. \quad (4.25)$$

In both Eqs. (4.23) and (4.25) we need the quantity $(\vec{0} | \mathcal{V} T_{B2} | \vec{0}) \vec{p}_2 \Big|_{\vec{P}_B=0}$ which, for the case of potential scattering, is easily obtained from a knowledge of the scattering cross section. For this case, using Eq. (4.5), we find

$$\tau_{\text{shear}} = \frac{1}{3mk_B T} \int d\vec{p}_2 \phi_2(p_2) \frac{p_2^3}{m} \int_0^\infty b db \int_0^{2\pi} d\psi (1 - \cos\theta), \quad (4.26)$$

where the scattering angle θ is given by

$$\cos\theta \equiv \vec{p}_2 \cdot \vec{p}_2^* / p_2^2. \quad (4.27)$$

The cross section is given by³

$$\sigma(p_2, \theta) = \frac{b db}{\sin\theta d\theta} \quad (4.28)$$

and thus

$$\tau_{\text{shear}} = \frac{8\pi^2}{3m^2 k_B T} \int_0^\infty dp_2 \phi_2(p_2) p_2^5 \int_0^\pi d(\cos\theta) (1 - \cos\theta) \sigma(p_2, \theta). \quad (4.29)$$

Similarly, using Eq. (4.24),

$$\mathcal{J} = \frac{8\pi^2}{3m^2} \int_0^\infty dp_2 \phi_2(p_2) p_2^5 \left[\frac{p_2^2}{2m} - \frac{5}{2} k_B T \right] \int_0^\pi d(\cos\theta) (1 - \cos\theta) \sigma(p_2, \theta). \quad (4.30)$$

It is generally accepted that the dynamics of the host-gas– B -particle collisions cannot be described solely in terms of potential scattering. Processes which lead to energy accommodation and diffuse scattering (e.g., roughness) are likely to be important. In order to include such processes here, we rewrite^{3(c)}

$$\phi_2(p_2) (\vec{0} | \mathcal{V} T_{B2} | \vec{0}) \vec{p}_2 = - \int_{|\hat{R}|=R} d^2\hat{R} \int d\vec{p}'_2 [K(\vec{p}'_2 \rightarrow \vec{p}_2 | \hat{R}) \vec{p}'_2 \phi_2(p'_2) - K(\vec{p}_2 \rightarrow \vec{p}'_2 | \hat{R}) \vec{p}_2 \phi_2(p_2)], \quad (4.31)$$

where $K(\vec{p}'_2 \rightarrow \vec{p}_2 | \hat{R})$ is the probability density per unit time that particles with momentum \vec{p}'_2 initially, leave the B particle with momentum \vec{p}_2 after a collision at unit vector \hat{R} on the B surface. This form can be used in Eqs. (4.22) and (4.25) in order to obtain τ_{shear} and \mathcal{J} once K is specified. Clearly, for nonpotential scattering, there is a great deal of freedom in choosing K . Nonetheless, some conditions can be imposed; for example,

$$K(\vec{p}'_2 \rightarrow \vec{p}_2 | \hat{R}) = 0 \quad (4.32)$$

for

$$\hat{R} \cdot \vec{p}'_2 > 0 \text{ or } \vec{p}_2 \cdot \hat{R} < 0,$$

detailed balance,

$$\begin{aligned} \phi_2(p'_2) K(\vec{p}'_2 \rightarrow \vec{p}_2 | \hat{R}) \\ = \phi_2(p_2) K(-\vec{p}_2 \rightarrow -\vec{p}'_2 | \hat{R}) \end{aligned} \quad (4.33)$$

and normalization,

$$\frac{|\vec{p}_2 \cdot \hat{R}|}{m} = \int d\vec{p}_2 K(\vec{p}'_2 \rightarrow \vec{p}_2 | \hat{R}), \quad \hat{R} \cdot \vec{p}'_2 < 0. \quad (4.34)$$

[See Ref. 3(c), Chap. III for a discussion of these symmetries.]

The use of an inelastic scattering mechanism in K does not follow from the theory presented here. We had assumed that B 's internal degrees of freedom separated from the rest. The use of an inelastic scattering kernel represents the opposite limit; that is, the internal degrees of freedom behave in a stochastic manner. This is therefore an additional phenomenological assumption in the theory [see Ref. 3(c) for a more detailed discussion of this point]. Before specifying K further, we return to τ_{shear} and \mathcal{J} .

If the B -gas interaction is taken to be that of elastic hard spheres ($\sigma = R^2/4$), we can easily evaluate the integrals in Eqs. (4.29) and (4.30) with the result that

$$\tau_{\text{shear}} = \left[\frac{8\pi k_B T}{m} \right]^{1/2} \frac{4R^2}{3} \quad (4.35a)$$

and

$$\mathcal{J} = \left[\frac{8\pi k_B T}{m} \right]^{1/2} \frac{2R^2}{3} (k_B T)^2. \quad (4.35b)$$

Scaling the more general scattering law expressions by the hard-sphere results gives

$$\tau_{\text{shear}} = \left[\frac{8\pi k_B T}{m} \right]^{1/2} \frac{4}{3} R^2 \Omega^{(1,1)*} \quad (4.36a)$$

and

$$\mathcal{J} = \left[\frac{8\pi k_B T}{m} \right]^{1/2} \frac{2}{3} R^2 (k_B T)^2 (6\Omega^{(1,2)*} - 5\Omega^{(1,1)*}) \quad (4.36b)$$

where the reduced collision integrals are defined as

$$\Omega^{(1,s)*} = \frac{m}{R^{2(s+1)}(2mk_B T)^s + 1/2 2\pi^{1/2}} \int d\vec{p}_2 p_2^{2s-2} \vec{p}_2 \int_{|\vec{R}|=R} d^2\vec{R} \int d\vec{p}'_2 [K(\vec{p}_2 \rightarrow \vec{p}'_2 | \hat{R}) \vec{p}_2 \phi_2(p_2) - K(\vec{p}'_2 \rightarrow \vec{p}_2 | \hat{R}) \phi_2(p'_2) \vec{p}'_2]. \quad (4.37)$$

The collision integrals defined by Eq. (4.37) are the same as those introduced in Ref. 20.

In this work we adopt Cercignani's model^{3(c),8} for the transition probability in the B -gas atom scattering event. Namely, we let

$$K(\vec{p}' \rightarrow \vec{p} | \hat{R}) = \frac{|p_\perp| |p'_\perp|}{m 2\pi (mk_B T)^2 \alpha_\perp \alpha_\parallel (2 - \alpha_\parallel)} I_0 \left[\frac{(1 - \alpha_\perp)^{1/2} p_\perp p'_\perp}{\alpha_\perp mk_B T} \right] \times \exp \left[-\frac{[p_\perp^2 + (1 - \alpha_\perp) p'^2_\perp]}{2mk_B T \alpha_\perp} - \frac{[\vec{p}_\parallel - (1 - \alpha_\parallel) \vec{p}'_\parallel]^2}{\alpha_\parallel (2 - \alpha_\parallel) 2mk_B T} \right], \quad p'_\perp < 0, \quad p_\perp > 0 \quad (4.38)$$

where \perp and \parallel denote the components normal and parallel to the B surface at \hat{R} , respectively, and I_0 is a Bessel function. The parameters α_\perp and α_\parallel are accommodation coefficients for the part of the relative kinetic energy corresponding to motion in the \hat{R} direction and transverse momentum, respectively. As Cercignani has shown,^{3(c),8} Eq. (4.38) can be derived on the basis of a stochastic model. Moreover, Eq. (4.38) has been used to compute detailed angular scattering cross sections⁸ with good agreement with experiment. The accommodation coefficients must satisfy

$$0 < \alpha_\perp < 1, \quad 0 < \alpha_\parallel < 2, \quad (4.39)$$

in order that Eq. (4.34) hold. In addition, K defined by Eq. (4.38) satisfies detailed balance [cf. Eq. (4.33)].

When α_\parallel and α_\perp vanish, the scattering process reduces to elastic hard-sphere scattering (i.e., K becomes a δ function). What about using a more realistic potential? As is easily shown, if $R \gg \sigma$, the range of the true surface potential, then the details of the potential are unimportant since $p_\perp = -p'_\perp + O(\sigma/R)$ no matter what

the potential (assuming that it is short range and neglecting grazing collisions). When $\alpha_{||}$ or α_{\perp} becomes unity, this corresponds to full thermal accommodation in the $||$ or \perp directions. Finally, $\alpha_{||}=2$ corresponds to the $||$ momentum being completely reversed on impact, a situation which is related to the rough sphere scattering model.^{3(a)}

When Eq. (4.38) is used in Eq. (4.37) we find (see Appendix B for the details)

$$\Omega^{(1,1)*} = 1 + \frac{1}{2}(\alpha_{||}-1) + \frac{\pi}{8}F\left[-\frac{1}{2}, -\frac{1}{2}; 1; (1-\alpha_{\perp})\right] \quad (4.40a)$$

and

$$\Omega^{(1,2)*} = 1 + \frac{1}{2}(\alpha_{||}-1) + \frac{\pi}{8}\left\{\frac{1}{2}F\left[-\frac{3}{2}, -\frac{1}{2}; 1; (1-\alpha_{\perp})\right] + \frac{1}{3}F\left[-\frac{1}{2}, -\frac{1}{2}; 1; (1-\alpha_{\perp})\right]\right\}, \quad (4.40b)$$

where F is a hypergeometric function. Using these results in Eqs. (4.36a) and (4.36b) gives

$$\tau_{\text{shear}} = \frac{4\pi R^2 \bar{c}}{3} \left[1 + \frac{1}{2}(\alpha_{||}-1) + \frac{\pi}{8}F\left[-\frac{1}{2}, -\frac{1}{2}; 1; (1-\alpha_{\perp})\right] \right] \quad (4.41a)$$

and

$$\mathcal{J} = \frac{2\pi R^2 (k_B T)^2 \bar{c}}{3} \left[1 + \frac{1}{2}(\alpha_{||}-1) + \frac{3\pi}{8}\left\{F\left[-\frac{3}{2}, -\frac{1}{2}; 1; (1-\alpha_{\perp})\right] - F\left[-\frac{1}{2}, -\frac{1}{2}; 1; (1-\alpha_{\perp})\right]\right\} \right]. \quad (4.41b)$$

In the last two expressions, the mean speed

$$\bar{c} \equiv \left(\frac{8k_B T}{\pi m} \right)^{1/2} \quad (4.42)$$

was introduced. Combining Eqs. (4.41a), (4.41b), and (4.22) gives

$$\tilde{V}_T = \frac{\lambda}{5p_h} \left[\frac{1 + \frac{1}{2}(\alpha_{||}-1) + \frac{3\pi}{8}\left\{F\left[-\frac{3}{2}, -\frac{1}{2}; 1; (1-\alpha_{\perp})\right] - F\left[-\frac{1}{2}, -\frac{1}{2}; 1; (1-\alpha_{\perp})\right]\right\}}{1 + \frac{1}{2}(\alpha_{||}-1) + \frac{\pi}{8}F\left[-\frac{1}{2}, -\frac{1}{2}; 1; (1-\alpha_{\perp})\right]} \right], \quad (4.43)$$

where $p_h = n_f k_B T$ is the ideal gas pressure. It is interesting to note that if we let

$$a \equiv \frac{\left\{4F\left[-\frac{1}{2}, -\frac{1}{2}; 1; (1-\alpha_{\perp})\right] - 3F\left[-\frac{3}{2}, -\frac{1}{2}; 1; (1-\alpha_{\perp})\right]\right\}}{1 + \frac{1}{2}(\alpha_{||}-1) + \frac{3\pi}{8}\left\{F\left[-\frac{3}{2}, -\frac{1}{2}; 1; (1-\alpha_{\perp})\right] - F\left[-\frac{1}{2}, -\frac{1}{2}; 1; (1-\alpha_{\perp})\right]\right\}}, \quad (4.44)$$

then Eq. (4.43) is identical with the result obtained by Waldmann⁶ for the thermophoretic velocity, although at the level of the scattering kernels K , the theories are still quite different.

The thermophoretic force is easily obtained once the friction constant is known [cf. Eqs. (4.16) and (4.13)]. Using Eq. (4.41a) we find that

$$\xi^{-1} = \frac{k_c}{3\pi^2 \eta} + \frac{1}{\rho_f \frac{4\pi R^2 \bar{c}}{3} \left[1 + \frac{1}{2}(\alpha_{||}-1) + \frac{\pi}{8}F\left[-\frac{1}{2}, -\frac{1}{2}; 1; (1-\alpha_{\perp})\right] \right]}. \quad (4.45)$$

At very low density, only the second term on the rhs of Eq. (4.45) is important (i.e., the Boltzmann limit). Unlike before, introducing a via Eq. (4.44) does not yield Waldmann's expression for the friction in the Boltzmann limit except for total ($\alpha_{\perp} = \alpha_{||} = 1$) or no accommodation.

In order to facilitate comparison with experiment, we introduce scaled velocity, friction, and thermophoretic force by scaling these quantities by their Boltzmann limit values when B is a hard sphere. Thus

$$V^* \equiv \bar{V}_T \frac{5p_h}{\lambda}, \quad (4.46a)$$

$$\xi^{*-1} \equiv \frac{4R^2 k_c \bar{c} \rho_f}{9\pi\eta} + \frac{1}{\left[1 + \frac{1}{2}(\alpha_{||} - 1) + \frac{\pi}{8} F\left[-\frac{1}{2}, -\frac{1}{2}; 1; (1 - \alpha_1)\right] \right]}, \quad (4.46b)$$

and

$$F^* \equiv \xi^* V^*. \quad (4.46c)$$

Notice that unlike Waldmann⁶ we, in general, do not have $F^*=1$. In addition, unlike Mason and Chapman⁷ (who assumed a diffuse scattering mechanism), we do not have $V^*=1$.

We are still faced with the problem of determining the accommodation coefficients $\alpha_{||}$ and α_1 . They are expected to be more or less independent of ρ_f , unless ρ_f is made so low that any adsorbed gas molecules desorb. We are not interested in this regime and thus by choosing the density to be sufficiently low so that the ring corrections can be omitted we, in principle, can determine $\alpha_{||}$ and α_1 from velocity and force measurements. Of course, a better way would be to have detailed angular patterns for molecular beam scattering from a surface of the material making up B and comparing with the patterns calculated by using the scattering kernels, Eq. (4.38). Since $\alpha_{||}$ enters into the expressions in a simple way, α_1 can be determined by noting that

$$\lim_{\substack{\rho_f \rightarrow 0 \\ \alpha_{||}, \alpha_1 \text{ const}}} F^* \left[\frac{1}{V^*} - 1 \right] = \frac{\pi}{8} \{ 4F\left[-\frac{1}{2}, -\frac{1}{2}; 1; (1 - \alpha_1)\right] - 3F\left[-\frac{3}{2}, -\frac{1}{2}; 1; (1 - \alpha_1)\right] \}. \quad (4.47)$$

This function is plotted in Fig. 2. In the next section we compare our theory with experiment.

V. COMPARISON TO EXPERIMENT

In the previous sections we have shown that the thermophoretic forces and velocities depend on the heat conductivity of the host gas, the pressure, the temperature, and the temperature gradient. A part of these quantities are control parameters in the actual experiments and the others can be easily measured independently. In addition, there are the two

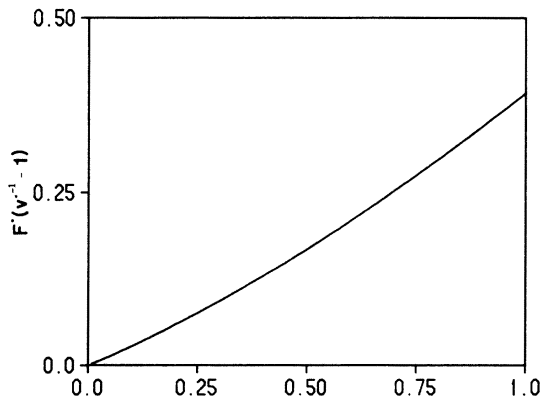


FIG. 2. Combination of the scaled force and velocity which leads to an unambiguous determination of α_1 in Cercignani's model for gas-surface scattering in the Boltzmann limit [see Eq. (4.47)].

accommodation coefficients which can be extracted, in principle, from molecule-surface scattering data. However, we are not aware of experiments in which the surface materials were the same as those making up the B particles. In addition, the pressures in surface scattering experiments are many orders of magnitude smaller than those typifying thermophoretic measurements, and thus the nature of the B surface may be quite different. Finally, there is the parameter k_c whose value in a dense gas is determined by the nature of the hydrodynamic boundary conditions: free (slip) or rigid (stick).

For the sake of comparison to experiment it is convenient to introduce a reduced force, defined by the ratio of the actual force to $R^2 \nabla T$. The reason is that the reduced force depends, for a given α_1 , $\alpha_{||}$, and T only on the ratio l/R . This can be seen from Eqs. (4.43), (4.45), and the low-density formulas for the heat conductivity and the pressure. A consequence of this property is that the reduced forces corresponding to different values of R should lie on a single curve, as a function of l/R . This consequence is born out experimentally as seen in all the figures (3–6) (when one disregards scatter in the experimental data).

Before comparing the theory with experiment, we wish to analyze the role of the parameter k_c . Figure 3 is a plot of the reduced force versus l/R for

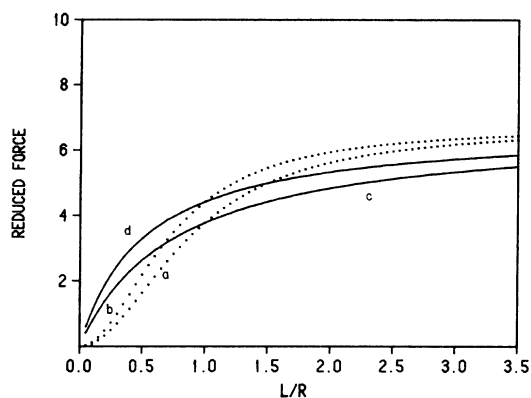


FIG. 3. Reduced force $[F_{Th}/(R^2\nabla T)\times 10^2$ in cgs] as a function of l/R . The curves labeled $a-d$ correspond to values of $k_c=3\pi/4l$, $3\pi/6l$, $3\pi/4R$ (slip), $3\pi/6R$ (stick), respectively. In all cases, the host gas was air at 307 K, $\alpha_{\perp}=1.0$, and $\alpha_{\parallel}=0.5$. Notice the small difference between the choice of slip (a,c) and stick (b,d) and the more rapid approach to the Boltzmann limit when $k_c\sim 1/l$.

different values of the cutoff parameter k_c . The material parameters correspond to air as a host gas (see Table I). The (dotted) curve a corresponds to $k_c=3\pi/4l$, the (dotted) curve b corresponds to $k_c=3\pi/6l$, curve c to $k_c=3\pi/4R$, and curve d to $k_c=3\pi/6R$. Thus curves c and d are constructed so that the friction attains its Stokes value for free and rigid boundary conditions, respectively [see Eq. (4.15)]. Curves a and b correspond to choosing the cutoff appropriate to the dilute ($l>R$) region (see Sec. IV), extrapolated beyond their range of validity. Their numerical prefactors ($3\pi/4$ or $3\pi/6$) have been chosen to match c,d at $l=R$. We see that the use of $k_c\sim 1/l$ causes the approach to the Boltzmann limit (when $l/R\rightarrow\infty$) to be faster than when $k_c\sim 1/R$. On the other hand, there is only a small difference between $k_c=3\pi/4$ or $3\pi/6$ corresponding to slip or stick, respectively. According to Sec. IV we must choose $k_c\sim O(1/l)$ as a cutoff when $l>R$ and $k_c\sim O(1/R)$ when $R>l$. This corresponds to choosing the pair of curves (a,c) for

TABLE I. Data (cgs) used for the comparisons with experiment.

	Air	Ar
T	307 K	299 K
∇T		49.4 K/cm
η	1.85×10^{-4}	2.27×10^{-4}
λ	1987 ^a	1770

^aThis is just the translational part of the thermal conductivity, $\lambda_{trans}\equiv 15k_B\eta/4m$.

$l>R$ and $l<R$, respectively, or the pair (b,d). Since curve a for $l>R$ and curve c for $l>R$ do not connect smoothly [the same holding for (b,d)], one gets a break in the curve, which is merely a reflection of the breakdown of the theory at $l=R$. In Figs. 4–6 we smooth this break (dashed lined) by interpolating between the $l>R$ and $l<R$ regions. In addition, we use “stick” boundary conditions, since these seem to be consistent with accommodation processes. It is worthwhile mentioning that the heat conductivity λ used in generating the graphs, for molecular host gases, includes an Eucken correction³ so that λ contains only the translational contribution. This is consistent with our assumption (see I) concerning the separability of internal degrees of freedom. The value of the mean free path is deduced, in all the experiments we refer to, from the viscosity η of the host gas via the formula

$$\eta = \frac{5\pi}{32}\rho\bar{c}l, \quad (5.1)$$

where ρ,\bar{c},l are defined in the previous sections.

Now we turn to actual experimental results. Schmidt^{2(a)} performed measurements of the thermophoretic forces and velocities for silicone oil droplets in argon. The relevant experimental parameters are given in Table I. For a given temperature and temperature gradient the measured thermophoretic velocity is independent of the particle radius R and is a function only of the mean free path l (in accordance with our theory). We find, using Schmidt’s data for \tilde{V}_T vs l that

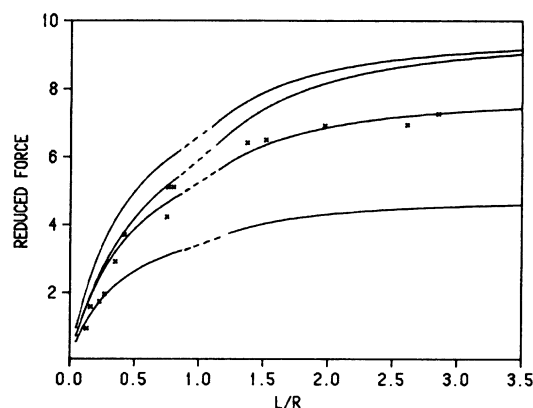


FIG. 4. Reduced force for silicone oil droplets in Ar at 299 K. The experimental points are due to Schmidt [Ref. 2(a)]. The solid curves result from our theory for pairs of $(\alpha_{\perp},\alpha_{\parallel})$ accommodation coefficients (from top to bottom) equal to (0,0), (1,1), (0.78, 0.37), and (1,0), respectively. The best fit ($\alpha_{\perp}=0.78$, $\alpha_{\parallel}=0.37$) resulted from the independent thermophoretic velocity experiment and the lowest-density force measurement.

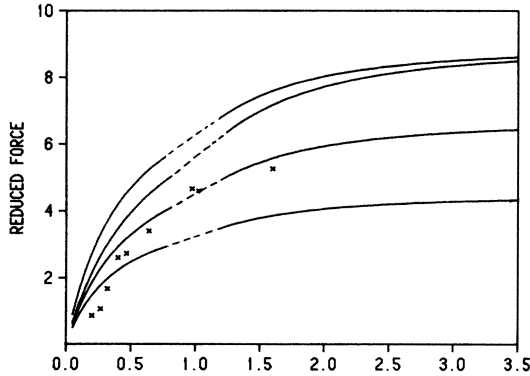


FIG. 5. Reduced force in air at 307 K. For pairs $(\alpha_{\perp}, \alpha_{\parallel}) = (0,0)$, $(1,1)$, $(1,0.5)$, and $(1,0)$ from top to bottom, respectively. The experimental points due to Schadt and Cadle [Ref. 2(b)] are for NaCl.

$$V_T = 0.18 \times 10^4 l \quad (5.2)$$

in cgs units. This means that

$$V_T^* \approx 0.79 . \quad (5.3)$$

Schmidt's experimental values of the force are depicted as x 's in Fig. 4.

In order to obtain the value of α_{\perp} we have used the value of the force F at the lowest measured density (rightmost x in Fig. 4). We then computed $F^*[(1/V^*) - 1]$. As explained in the preceding section, this expression depends only on α_{\perp} . Figure 4 shows the dependence of $F^*[(1/V^*) - 1]$ on α_{\perp} . Thus, we find that $\alpha_{\perp} = 0.78$. Next, we used Eq. (4.46) and the observed value of V^* to find α_{\parallel} , with the result that $\alpha_{\parallel} = 0.37$. From atom-surface scattering data,^{3(c)} a difference in α_{\parallel} and α_{\perp} is to be expected, the latter usually being larger. Using these parameters we have calculated the reduced force l/R . The result is plotted in Fig. 3 (second

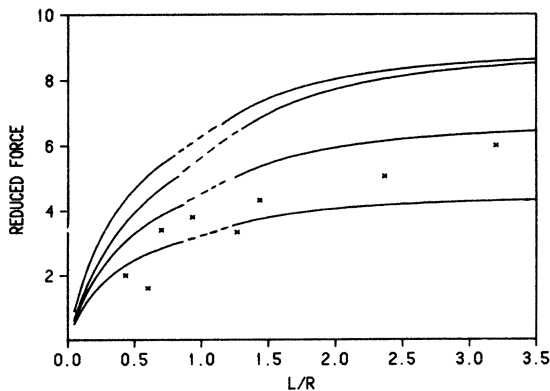


FIG. 6. Same as Fig. 4, except that now the experimental points are for Hg.

curve from the bottom). The agreement with experiment is good. For comparison, we also plotted the reduced force for other values of the accommodation coefficients. The top curve corresponds to $\alpha_{\perp} = \alpha_{\parallel} = 0$, i.e., a hard-sphere potential and no accommodation. Second from the top is the case $\alpha_{\perp} = \alpha_{\parallel} = 1$ corresponding to full accommodation. In the limit of zero density ($l/R \rightarrow \infty$) both the top curve and the curve next to it reduce to the hard-sphere result for the force. This is also Waldmann's result. As is obvious from the experimental data the actual force is smaller than the hard-sphere value. The bottom curve corresponds to $\alpha_{\perp} = 1$ and $\alpha_{\parallel} = 0$, i.e., no longitudinal accommodation. This curve lies below the experimental data and in fact is the lowest possible curve obtainable from our theory. We wish to stress that the best-fitting curve is not a fit, since we have deduced the accommodation parameters on the basis of a *single point* on that curve and the velocity data.

The obvious crossover of the force from a low-density behavior ($l > R$, reduced force $\rightarrow_{l \rightarrow \infty} \text{const}$) to a high-density behavior is due to the crossover of the friction coefficient from its value predicted by the Boltzmann equation to the Stokes value. The fact that our interpolation between the dilute Boltzmann limit and the Stokes limit works so well can be taken as support of the repeated-ring approximation.

As mentioned in the preceding section when $l \rightarrow \infty$, $F^* - \frac{1}{2}\alpha_{\parallel}$ is a function of α_{\perp} alone [see Eqs. (4.43) and (4.46)]. A numerical calculation of the hypergeometric functions that appear in these equations shows that $F^* - \frac{1}{2}\alpha_{\parallel}$ is a monotonously decreasing function of α_{\perp} bounded by

$$0.5 \leq F^* - \frac{1}{2}\alpha_{\parallel} \leq 1 . \quad (5.4)$$

Since $0 \leq \alpha_{\parallel} \leq 2$ we obtain bounds for F^* :

$$0.5 \leq F^* \leq 2 . \quad (5.5)$$

The upper bound is achieved when $\alpha_{\parallel} = 2$ and $\alpha_{\perp} = 0$ and the lower bound is reached for $\alpha_{\parallel} = 0$ and $\alpha_{\perp} = 1$. In the same way it follows that

$$0.8927 \dots \leq V^* - \frac{\alpha_{\parallel}}{2} \leq 1 \quad (5.6)$$

or

$$0.8927 \dots \leq V^* \leq 2 .$$

Thus, if one believes the validity of the Cercignani model for accommodation, both the reduced thermophoretic velocity and force are bounded (when $l/R \rightarrow \infty$). The data available to us are compatible

with those bounds.

For comparison, we mention that if one uses energy accommodation (e.g., Waldmann's assumptions) one obtains $F^*=1$ and $V^* < 1$, which is in disagreement with experiment. Mason and Chapman's assumption of a diffuse scattering mechanism yield $V^*=1$ and $F^* > 1$, again in disagreement with experiment. We conclude that a correct choice of the accommodation mechanism is extremely important for the understanding of the thermophoretic data. Moreover, the sensitivity of the experiment to accommodation coefficients suggests that such experiments can be used to measure accommodation coefficients in relatively dense gases, where standard beam experiments do not work. (Beam experiments are at pressures much less than 1 torr whereas thermophoresis experiments can be done even at pressures of hundreds of atmospheres.)

Figures 5 and 6 correspond to thermophoretic forces acting on particles with high heat conductivity. Figure 5 shows the experimental data of Schadt and Cadle for NaCl particles in air at 307 K and a temperature gradient of ~ 49.4 K. Figure 6 shows similar measurements for mercury particles in air. Unfortunately, we know of no velocity measurements in these cases. F^* in this case is ~ 0.54 , so it is close to its lower bound [Eq. (5.4)]. This corresponds to $\alpha_1 \approx 1$. Indeed, the two lowest curves, having $\alpha_1=1$ and $\alpha_{||}=0$ and 0.5 (from bottom to top) seem to be in good agreement with experiment. It is interesting to note that Epstein's theoretical prediction in this case is about 30 times too small.²¹ This is so because his formula overestimates the role of the internal heat conductivity of the particles. In fact, it seems from our agreement with experiment that this internal heat conductivity can play only a minor role, at least when the density of the host gas is not too high. The theoretical reason has been given in the previous sections.

In conclusion, our theory is in good agreement with experiment. The latter seems to be sensitive to the accommodation processes but not to the internal heat conductivity of the particles. It is important to perform more experiments and measure *both* the thermophoretic forces and velocities. In addition, independent measurements of the accommodation coefficients, for example, by molecule-surface scattering, may eliminate the remaining two parameters appearing in our theory.

VI. DISCUSSION

We have shown that thermophoresis, although being a macroscopic, nonfluctuating effect is of

nonhydrodynamic origin. Firstly, the linearized Navier-Stokes equation (with the usual boundary conditions) predicts no thermophoresis. This solution is stable to nonlinear perturbations. Secondly, the fluctuating hydrodynamic equations (mode coupling) yields a vanishingly small renormalization of the bare thermophoretic effect. This is consistent with the low-density results, but is not very useful. Finally, kinetic theory shows that the effect is of kinetic origin and is not renormalized by higher-order (ring) or correlated events, which are typical of the hydrodynamic regime. We have also shown that the observed thermophoretic force changes its behavior as one moves from a dilute host gas to a denser host gas. This change reflects the crossover of the friction coefficient from its Boltzmann value to its Stokes value.

The guest B particle can be grossly described by a hard-sphere potential. The use of such a potential yields results which are in qualitative order of magnitude agreement with experiments. To achieve a better fit of the data one needs a more detailed description of the interactions between the guest particle and the host-gas particles. It turns out that a small attractive potential tail, which is always present is not significant as far as thermophoresis is concerned. The reason is that the typical range of such a potential is angstroms whereas the typical size of the guest particle is about a μm . Another mechanism of relevance to the scattering of host molecules of the guest particle is accommodation. We have shown that the simplest accommodation models cannot possibly account for the data.^{6,7} Only when a more sophisticated model, allowing different degrees of accommodation for transverse and longitudinal components of momenta, is introduced can one achieve a good fit to the data. Indeed, the sensitivity of thermophoretic phenomena to the details of the gas-surface scattering process, suggests that thermophoretic measurements could be used to experimentally determine the accommodation coefficients. This takes place in density regimes many orders of magnitude too large for conventional "beam" experiments to be of much use.

We stress that unlike in Epstein's formula, the internal heat conductivity of the guest particle does not appear in our formulas. This is because we did not directly take internal degrees of freedom into account. They were included phenomenologically through the accommodation mechanism. On the other hand, as explained by Waldmann,²¹ this internal conductivity is unimportant for dilute enough host gases. This is because the particle does not

stay for a large enough time in any region in space in order to equilibrate with its surroundings. Thus, Epstein's formula cannot be right (and indeed does not compare well with experiments) for highly conducting particles. In the case of a dense host fluid (or a liquid) one in general cannot neglect the internal degrees of freedom of the guest particle. This case is quite complicated and no microscopic theory of thermophoresis, valid in the dense fluid regime, is known to us.

On a more general level, we have shown that the thermophoretic force coefficient is related in a simple way to the Soret coefficient. Since it is well known that the latter is sensitive to microscopic details (i.e., scattering laws), so is the thermophoretic force coefficient.

There are several approximations in our work. One of them was mentioned before: the neglect of internal degrees of freedom of the guest particle. Another approximation is the use of the lowest order Sonine polynomial expansion in solving the integral equations associated with the repeated-ring approximation. Only in this approximation do the repeated-ring corrections exactly cancel in \tilde{V}_T . Higher-order corrections in the Sonine polynomials will renormalize both the velocity and the force. Such a (multiplicative) correction will have the form

$$\frac{1 + c_1 \frac{R}{l} + c_2 \left[\frac{R}{l} \right]^2 + \cdots}{1 + c_3 \left[\frac{R}{l} \right] + c_4 \left[\frac{R}{l} \right]^2 + \cdots},$$

the c_i 's being constants. As l decreases (denser gas) the result will tend to c_1/c_3 of the lowest order result (assuming $c_1 \gg c_2, c_3 \gg c_4$), then c_2/c_4 of it, etc. Such a qualitative change is indeed observed in some experiments.²¹ Still another approximation is the neglect of the k dependence of the binary collision operators and the introduction of a cutoff k_c to compensate for this approximation. It has been shown in the case of Stokes friction that such a procedure can yield qualitatively correct results.^{5,22} A more severe error associated with k_c is the hydrodynamic approximation, whereby only the hydrodynamic part of the operators, as well as the small- k forms of the hydrodynamic eigenvalues are kept. This has the advantage that analytic results can be obtained. As discussed in Sec. IV, the cutoff is $O(\min\{1/R, 1/l\})$. The precise numerical factors are important as far as free (slip) versus rigid (stick) boundary conditions are concerned. However, the thermophoretic force seems to be relatively insensi-

tive to the choice of these boundary conditions. What does matter, however, is the point where the cutoff changes from one behavior to the other. We have chosen $l=R$ for the transition. At this point one gets a break in the approximate curves describing the force versus l/R , which merely indicates the fact that the theory breaks down for $l \sim R$, in the absence of a small parameter. One can eliminate the need for k_c in a numerical study and we are actively pursuing this direction.

Another approximation is the inclusion of only ring and repeated-ring events. This involves neglecting ring within ring, three-body collisions, etc. These events should yield well-behaved higher-order (in density) corrections although their relative importance is unknown. In addition, we have neglected static correlations. This is reasonable for a dilute enough host gas, although certainly not for a liquid.^{2(c)} Finally, for large enough temperature gradients, nonlinear terms in ∇T should be considered.

We feel that the next step should be a better kinetic treatment (perhaps a numerical one) where some of our approximations can be relaxed. A promising method seems to be the variational approach.

Internal degrees of freedom should be taken into account as a first step towards understanding thermophoresis in dense fluids. Finally, since the B particles in experiments may be charged one should investigate the effect of charge on thermophoresis.

Since the existing experiments rarely measure the forces and velocities separately, we believe that many experiments should be performed in order to measure the dependence of thermophoresis on the physical properties of the host fluid and the guest particles. In addition, independent gas-surface scattering measurements would be very useful in providing a qualitative check of the accommodation coefficients deduced from thermophoretic experiments, although, as mentioned above, one should exercise some care in comparing beam data ($p_h \sim 10^{-8}$ torr) with thermophoretic data ($p_h \sim 10^2$ torr).

ACKNOWLEDGMENTS

A portion of this work was supported by a Cottrell Research Grant from the Research Corporation. The authors would like to thank J. R. Dorfman, R. G. Gordon, and G. M. McClelland for useful discussions. One of us (I.G.) acknowledges support from the National Science Foundation under Grant No. CHE-79-23235.

APPENDIX A

In this appendix we show that the exchange rings are negligible. Physically we expect this to be the case since they involve two bath particles in a coherent way (i.e., both must collide with B). The contribution of the exchange rings to \tilde{V}_T [cf. Eq. (3.19)] is

$$\begin{aligned}
 (\tilde{V}_T)_{\text{ex}} &= \frac{-\rho_f^2}{m^2 M k_B T^2} \int d\vec{P}_B d\vec{p}_2 d\vec{p}_3 \phi_B(P_B) \phi_2(p_2) \phi_3(p_3) \vec{P}_B \mathcal{G}_B^{(1)}(s) \\
 &\quad \times \left[\vec{0} \left| \frac{1}{1 + \mathcal{V} T_{B2} \mathcal{G}_{B2}} \mathcal{V} T_{B2} \mathcal{G}_{B2} \mathcal{V} T_{B3} \mathcal{G}_{23} \mathcal{V} T_{23} (1 + \mathcal{P}_{23}) \right| \vec{0} \right] \frac{1}{(s - n_f \mathcal{L}_f)} \\
 &\quad \times \frac{\vec{p}_2}{m} \left[\frac{p_2^2}{2m} - \frac{5}{2} k_B T \right], \quad s \rightarrow 0+.
 \end{aligned} \tag{A1a}$$

Carrying out the one Sonine polynomial expansions described in the text yields

$$\begin{aligned}
 (\tilde{V}_T)_{\text{ex}} &\approx \frac{-2\rho_f \lambda}{5\xi(k_B T)^3} \int d\vec{P}_B d\vec{p}_2 d\vec{p}_3 \phi_B(P_B) \phi_2(p_2) \phi_3(p_3) \vec{P}_B \\
 &\quad \times \left[\vec{0} \left| \frac{1}{1 + \mathcal{V} T_{B2} \mathcal{G}_{B2}} \mathcal{V} T_{B2} \mathcal{G}_{B2} \mathcal{V} T_{B3} \mathcal{G}_{23} \mathcal{V} T_{23} (1 + \mathcal{P}_{23}) \right| \vec{0} \right] \frac{\vec{p}_2}{m} \left[\frac{p_2^2}{2m} - \frac{5}{2} k_B T \right].
 \end{aligned} \tag{A1b}$$

The combination of operators $(1 + \mathcal{V} T_{B2} \mathcal{G}_{B2})^{-1} \mathcal{V} T_{B2}$ is exactly the same as what appears in $\mathcal{G}_B^{(1)}(s)$, although we do not consider only the $(\vec{0} | | \vec{0})$ matrix element. On the other hand, since we neglect the k dependence of the T 's and will evaluate the expressions within the context of the lowest-order hydrodynamic approximation, we can write

$$\vec{P}_B \left[\vec{0} \left| \frac{1}{(1 + \mathcal{V} T_{B2} \mathcal{G}_{B2})} \mathcal{V} T_{B2} \right| \vec{k}, -\vec{k} \right] \approx \frac{\xi}{n_f} \left[\frac{\vec{P}_B}{M} - \frac{\vec{p}_2}{m} \right], \tag{A2}$$

and hence Eq. (A2) becomes

$$\begin{aligned}
 (\tilde{V}_T)_{\text{ex}} &\approx \frac{-2m\lambda}{5M(k_B T)^3} \int d\vec{P}_B d\vec{p}_2 d\vec{p}_3 \phi_B(\vec{P}_B) \phi_2(\vec{p}_2) \phi_3(\vec{p}_3) \left[\vec{P}_B - \frac{M}{m} \vec{p}_2 \right] \\
 &\quad \times \int_{k < k_c} \frac{d\vec{k}}{(2\pi)^3} (\vec{k}, -\vec{k} | \mathcal{G}_{B2} \mathcal{V} T_{B3} \mathcal{G}_{23} \mathcal{V} T_{23} (1 + \mathcal{P}_{23}) | \vec{0}) \frac{\vec{p}_2}{m} \left[\frac{p_2^2}{2m} - \frac{5}{2} k_B T \right],
 \end{aligned} \tag{A3}$$

where, as in the text, ξ has canceled. Of the two terms on the rhs of Eq. (A2), only the one in \vec{P}_B is important. Since \vec{p}_2 is the lowest-order shear eigenmode (it can be shown that the longitudinal contribution is much less important), $\vec{p}_2 \mathcal{G}_{B2} \propto \vec{p}_2$. On the other hand, $\vec{p}_2 T_{B3}$ vanishes and thus the term in \vec{p}_2 makes no contribution in the lowest-order hydrodynamic approximation.

A crude estimate is now sufficient to show that $(\tilde{V}_T)_{\text{ex}}$ is negligible. The operator appearing in Eq. (A3) is singular as $k \rightarrow 0$. The singularity results from the hydrodynamic parts of the propagators

$\mathcal{G}_{B,2}$ and $\mathcal{G}_{2,3}$. The latter will behave as

$$\mathcal{G}_{23} \sim (vk^2)^{-1}, \quad k < k_c \tag{A4}$$

while

$$\mathcal{G}_{B,2} \sim (\xi_B/M)^{-1}, \quad k < k_c. \tag{A5}$$

Unlike the analysis given in the text, we must keep \mathcal{L}_B in $\mathcal{G}_{B,2}$ since it protects part of the divergence at $k=0$. Moreover,

$$\vec{P}_B(0 | \mathcal{V} T_{B3} | \vec{0}) \sim mR^2 \bar{c}^2 \tag{A6}$$

and

$$(0 | VT_{23} | \vec{0}) \sim \bar{c} \sigma^2, \quad (\text{A7})$$

where the mean speed \bar{c} is given by Eq. (4.42) and R and σ are typical dimensions for the B and gas particles, respectively. Finally, inserting estimates for the size of $(\vec{p}_2/m)[(p_2^2/2m) - \frac{5}{2}k_B T]$ gives

$$(\tilde{V}_T)_{\text{ex}} \sim \lambda \frac{R^2 \sigma^2 k_c}{\xi_B \nu}, \quad (\text{A8})$$

since $\nu \sim l\bar{c}$, $\xi_B \sim mR^2 \bar{c} n_f$, and $k_c \sim \min(R^{-1}, l^{-1})$,

$$(\tilde{V}_T)_{\text{ex}} \sim \frac{\lambda}{nk_B T} \frac{\sigma^2}{l \max(R, l)}. \quad (\text{A9})$$

We are using kinetic theory and thus require that $\sigma \ll l$. Moreover, for our formalism to hold, we must consider a large B particle [i.e., $(m/M) \ll 1$ and $\sigma \ll R$]. Thus

$$\frac{\sigma^2 k_c}{l} \ll 1,$$

which implies that $(\tilde{V}_T)_{\text{ex}}$ is small with respect to \tilde{V}_T [cf. Eq. (4.43)].

APPENDIX B: DERIVATION OF EQS. (4.40a) AND (4.40b)

The integrations appearing in Eq. (4.37) are best considered in two parts. Using Eq. (4.34) we find

$$\frac{m}{R^{2(s+1)}(2mk_B T)^{s+(1/2)}2\pi^{1/2}} \int d\vec{p}_2 d\vec{p}'_2 p_2^{2(s+1)} \vec{p}_2 \cdot \int_{|\vec{R}|=R} d^2\vec{R} K(\vec{p}_2 \rightarrow \vec{p}'_2 | \hat{R}) \vec{p}_2 \phi_2(p_2) = 1. \quad (\text{B1})$$

The remaining term in Eq. (4.37) is equal to (we choose $m=1$)

$$\Lambda_s \equiv \frac{-2\pi^{1/2}}{(s+1)!(2k_B T)^{s+(1/2)}} \int_{\substack{p'_1 > 0 \\ p_1 < 0}} d\vec{p} d\vec{p}' (p_1^2 + \vec{p}_{||} \cdot \vec{p}'_{||})^{s-1} (\vec{p}_1 \cdot \vec{p}'_1 + \vec{p}_{||} \cdot \vec{p}'_{||}) \phi_2(\vec{p}_2) K(\vec{p}' \rightarrow \vec{p} | \hat{R}). \quad (\text{B2})$$

Following Cercignani^{3(c)} we note that [the reader should be aware that there are many misprints in Ref. 3(c)]

$$K(\vec{p}' \rightarrow \vec{p} | \hat{R}) = \left[\frac{2\pi}{k_B T} \right]^{1/2} \phi_2(p) |_{p_1 p'_1} \sum_{lmn} (1-\alpha_\perp)^l (1-\alpha_{||})^{m+n} \psi_{lmn}(\vec{p}) \psi_{lmn}(\vec{p}') \quad (\text{B3})$$

with

$$\psi_{lmn}(\vec{p}) = L_l \left[\frac{p_\perp^2}{2k_B T} \right] H_m \left[\frac{p_{||,1}}{\sqrt{2k_B T}} \right] H_n \left[\frac{p_{||,2}}{\sqrt{2k_B T}} \right] (2^m + n m! n!)^{-1/2}, \quad (\text{B4})$$

where L_l and H_m are Laguerre and Hermite polynomials, respectively. The functions ψ_{lmn} are orthogonal in the sense that

$$\{\psi_{lmn}, \psi_{l'm'n'}\} \equiv \left[\frac{2\pi}{k_B T} \right]^{1/2} \int_{p_1 > 0} d\vec{p} p_1 \phi_2(p) \psi_{lmn}(\vec{p}) \psi_{l'm'n'}(\vec{p}) = \delta_{l,l'} \delta_{m,m'} \delta_{n,n'}. \quad (\text{B5})$$

Using Eqs. (B3)–(B5) in (B2) gives for $s=1$

$$\Lambda_1 = \sum_{lmn} (1-\alpha_\perp)^l (1-\alpha_{||})^{m+n} (-1)^{m+n} \frac{(\{p_\perp, \psi_{lmn}\}^2 + 2\{p_{||,1}, \psi_{lmn}\}^2)}{4k_B T}, \quad (\text{B6})$$

where we have used the parity of the Hermite polynomials under inversion in writing the last expression. Since

$$p_{||,1} = \sqrt{k_B T} \psi_{010} \quad (\text{B7})$$

and noting that

$$\frac{1}{k_B T} \int_0^\infty dp_\perp p_\perp^{n+1} e^{-p_\perp^2/2} L_l(\beta p_\perp^2/2) = (2k_B T)^{n/2} \frac{\Gamma\left[\frac{n}{2}+1\right] \Gamma\left[l-\frac{n}{2}\right]}{l! \Gamma(-n/2)}, \quad (\text{B8})$$

we have

$$\Lambda_1 = \frac{1}{2}(\alpha_{||} - 1) + \frac{\pi}{8} \sum_l (1 - \alpha_l)^l \frac{\Gamma(l - \frac{1}{2})^2}{(l!)^2 \Gamma(-\frac{1}{2})^2} . \quad (\text{B9})$$

The series on the rhs of (B9) is a hypergeometric series. Hence, adding Eqs. (B1) and (B9) yields Eq. (4.40a). In essentially the same fashion, Eq. (4.40b) can be obtained, the details being left to the reader.

- ¹I. Goldhirsch and D. Ronis, Phys. Rev. A 27, 1616 (1983), preceding paper.
- ²See, e.g., (a) K. H. Schmitt, Z. Naturforsch. 14a, 870 (1959); (b) C. F. Schadt and R. D. Cadle, J. Phys. Chem. (Ithaca) 65, 1689 (1961); (c) G. S. McNab and A. Meisen, J. Colloid Interface Sci., 44, 339 (1973); (d) L. Talbot, R. K. Cheng, R. W. Schefer, and D. R. Willis, J. Fluid Mech. 101, 737 (1980).
- ³(a) S. Chapman and T. G. Cowling, *The Mathematical Theory of Non-uniform Gases*, 3rd ed. (Cambridge University Press, Cambridge, England, 1970); (b) P. Resibois and M. DeLeener, *Classical Kinetic Theory of Fluids* (Wiley, New York, 1977); (c) C. Cercignani, *Theory Application of the Boltzmann Equation* (Elsevier, New York, 1975).
- ⁴(a) M. H. Ernst and J. R. Dorfman, Physica (Utrecht) 61, 157 (1972); (b) J. R. Dorfman, in *Fundamental Problems in Statistical Mechanics*, edited by E. G. D. Cohen (North-Holland, Amsterdam, 1975), Vol. III; (c) J. R. Mchaffey and R. I. Cukier, Phys. Rev. A 17, 1181 (1978); (d) H. Van Beijeren and J. R. Dorfman, *ibid.* 19, 416 (1979).
- ⁵(a) J. R. Dorfman, H. Van Beijeren, and C. F. McClure, Arch. Mech. 28, 333 (1976); (b) H. Van Beijeren and J. R. Dorfman, J. Stat. Phys. 23, 335 (1980); 23, 443 (1981).
- ⁶L. Waldman, Z. Naturforsch. 14a, 589 (1959).
- ⁷E. A. Mason and S. Chapman, J. Chem. Phys. 36, 627 (1962).
- ⁸(a) C. Cercignani and M. Lampis, Trans. Theory 1, 101 (1971); (b) C. Cercignani, in *Rarefied Gas Dynamics*, edited by Dini *et al.* (Academic, New York, 1974), Vol. II, p. 75.
- ⁹A. J. F. Siegert and E. Teramoto, Phys. Rev. 110, 1232 (1958).
- ¹⁰R. Zwanzig, Phys. Rev. 129, 486 (1963).
- ¹¹For a review see M. H. Ernst, L. K. Haines, and J. R. Dorfman, Rev. Mod. Phys. 41, 296 (1969).
- ¹²See, e.g., K. Kawasaki and I. Oppenheim, Phys. Rev. 139A, 1763 (1965).
- ¹³J. R. Dorfman and E. D. G. Cohen, Phys. Rev. A 6, 776 (1972); 12, 292 (1975).
- ¹⁴D. Ronis, I. Procaccia, and I. Oppenheim, Phys. Rev. A 19, 1307 (1979).
- ¹⁵J. T. Bartis and I. Oppenheim, Physica (Utrecht) 74, 1 (1974).
- ¹⁶See, e.g., D. Ronis and I. Oppenheim, Physica (Utrecht) 84A, 620 (1976), and references therein.
- ¹⁷(a) J. M. J. Van Leeuwen and A. Weijland, Physica (Utrecht) 36, 457 (1967); 38, 35 (1968); (b) M. H. Ernst and A. Weyland, Phys. Lett. 34A, 39 (1971); (c) A. Weyland, J. Math. Phys. 15, 1942 (1974).
- ¹⁸A. J. Masters and T. Keyes, Phys. Rev. A 25, 1010 (1982).
- ¹⁹L. D. Landau and E. M. Lifshitz, *Fluid Mechanics* (Pergamon, New York, 1959).
- ²⁰J. O. Hirschfelder, C. F. Curtiss, and R. B. Bird, *Molecular Theory of Gases and Liquids* (Wiley, New York, 1964).
- ²¹See, e.g., the review by L. Waldmann and K. H. Schmitt, in *Aerosol Science*, edited by C. W. Davies (Academic, New York, 1966).
- ²²C. F. McClure, Ph.D. thesis, University of Maryland 1972 (unpublished).